The Geological Society Special Publications

Geochemical discrimination and petrogenetic affinities of dykes intruding the Ladakh batholith, NW India

--Manuscript Draft--

Manuscript Number:	GSLSpecPub17-150R3
Article Type:	Research article
Full Title:	Geochemical discrimination and petrogenetic affinities of dykes intruding the Ladakh batholith, NW India
Short Title:	Geochemical discrimination of Ladakh dykes
Corresponding Author:	Alexandra Regina Heri, Ph.D. University of Houston Houston, TX UNITED STATES
Corresponding Author E-Mail:	heri.alexandra@gmail.com;arheri@uh.edu
Other Authors:	Justin Bahl
	Igor Maria Villa
Order of Authors (with Contributor Roles):	Alexandra Regina Heri, Ph.D. (Conceptualization: Equal; Formal analysis: Lead; Methodology: Equal; Software: Supporting; Visualization: Lead; Writing – original draft: Lead; Writing – review & editing: Lead)
	Justin Bahl (Conceptualization: Equal; Formal analysis: Supporting; Methodology: Equal; Software: Lead; Validation: Equal; Writing – review & editing: Supporting)
	Igor Maria Villa (Conceptualization: Supporting; Methodology: Supporting; Writing – review & editing: Supporting)
Abstract:	Eocene dykes extending over 50 km along the southern margin of the Ladakh batholith (NW India) fall into two main groups showing different orientation as well as isotope and trace element geochemistry. Both dyke families formed in the same tectonic setting over a time span of approximately 4 Ma. However, each family is far from monolithic, and therefore we tested several statistical approaches to identify geochemical subgroups from REE data and relate them to magmatogenetic processes. Hierarchical Clustering and Multidimensional Scaling calculate similarities/dissimilarities among individuals of a population. Both statistical tools, when applied to the Ladakh dykes, reflect the east-west dichotomy. However, detailed quantification of the resulting grouping varies according to input data. Normalization to chondrites yields slightly different groupings from unnormalized concentration data. Population-internal REE normalization provides the most accurate grouping as revealed by the fact that multiple samples from the same dyke are assigned the closest relatedness. Independently from normalization, east-west dichotomy is mirrored by marked differences in degree of crustal assimilation and magma evolution, pointing to km-scale geological heterogeneity. Finally, dykes intruding the Ladakh batholith 150 km SE of the present samples are geochemically similar, but cluster as distinct group.
Section/Category:	Crustal Architecture and Evolution of the Himalaya-Karakoram-Tibet Orogen
Additional Information:	
Question	**Response**
Are there any conflicting interests, financial or otherwise?	No
Samples used for data or illustrations in this article have been collected in a responsible manner	Confirmed

Dear Editor in Chief

please find attached the R2 version of the manuscript GSLSpecPub17-150R1 by Heri et al.

The reviewers' reports have been taken into account as follows:

We thank reviewer 1 for the time he has spent on reading and reviewing our manuscript. We feel that there are misunderstandings we try to clarify in our answer.

If substantial metasomatism has taken place, and if this has substantially changed the major element composition, then the trace element concentrations can no longer be normalised to chondrites! Let me illustrate this with a simple numerical example.

We do understand the concerns of reviewer 1 based on the given example. However - his argument is based on numbers that cannot be reconciled with the determination of major and trace elements in practice. The reviewer's example is based on a 3-component system consisting of 1 major element and 2 trace elements. The observed decrease in chondrite-normalised trace element content between sample B and B' by 50% is based on a 100% increase in the mobile major element data due to the constant sum constraint, ie. the components have to add up to 1'000'000 ppm. The fallacy in this lies in the practice of major and trace element determination. Aitchison based his work exclusively on major element oxide data and we do agree that in the case of major element data, the constant sum constraint is a concern and Aitchison distances should be employed. However, trace elements are different. The total amount of trace elements is not reflected in major element data, since major elements are determined independently from trace elements. If we could resolve for the constant sum constraint as suggested in the example given by reviewer 1, the major element content would negatively correlate with the trace element content – the higher the total amount of trace elements measured in a rock sample, the lower the major element content should be – as it is the case in the example of rocks A and B given by reviewer 1. This is clearly not the case in reality. Trace element concentrations in a rock lie within the uncertainty of 1–5 wt% oxide for major element concentration values.
Furthermore, reviewer 1 states that "*If substantial metasomatism has taken place, and if this has substantially changed the major element composition, then the trace element concentrations can no longer be normalised to chondrites!".* Unfortunately, we do not know the unaltered rock compositions and can therefore not make a comparison between altered and an unaltered rocks. However, the example chosen by rewiewer 1 is unrealistically high. In fact, we consciously collected dyke 3 in three points of the same outcrop showing increasing degrees of visible alteration (Heri et al., 2015). The most extreme variations of soluble alkalis was -14 % (Heri et al, 2015, Table S2), and the matching increase of immobile Ti was +11 %; these variations are similar to the analytical reproducibility of REE concentration measurements. Moreover, the degree of autometamorphism observed strongly varies. Some dykes are very pristine while others show alteration of major mineral phases making major element comparisons less informative than focusing on REE. Typical REE host minerals such as apatite and sphene look generally pristine and were unlikely passively enriched or depleted in a way that would have substantially changed the REE concentrations in the rocks. We therefore believe it is extremely unlikely that the alteration we observed has led to changes in REE concentrations that would forbid the normalization to chondrite or any other reference material. We discuss the effect of different reference materials on HC and MDS in the paper. The comparison of elemental enrichment factors instead of elemental concentrations is nothing new –reviewer 1 seems to be confused by our attempt to compare REE patterns instead of elemental concentrations.

I am confused about the biplot that is shown under point 3 of the rebuttal. In the text immediately above this figure, the authors say that it shows a PCA plot of REE using relative abundances AND Aitchison distances. Which is it? I only see one biplot. Was this produced using relative abundances or Aitchison distances? It can't be both because relative chondrite normalised abundances are incompatible with Aitchison's logratio distances, as I have shown above.

We are very sorry for the confusion caused by our inadequate description of the given PCA figure. This biplot is exactly what reviewer 1 has suggested us to do – the concentrations were NOT normalized to any reference material. This is the PCA biplot of REE concentrations using Aitchison's logratio distances. We used HC and MDS of REE enrichment factors to find the most similar samples based on REE patterns – we feel that we have found a way to achieve this. The PCA biplot using Aitchison distances however, does not cluster the dykes in a way that satisfies our sanity checks. The REE patterns that are the most similar because they originate from the same dyke or dykes that originate from the same magma (dyke 3 and dyke U&V, respectively) do not cluster. We understand the reviewer's concerns but feel like our method manages to find the most similar REE patterns out of many as shown in figures 11 and 12. Our approach was derived empirically and we admittedly do not understand all the details of the analysis, but the arguments of reviewer 1 that our approach is fundamentally flawed because we have not used PCA and Aitchison's logratio distances is not convincing to us since our approach clusters the dykes with the most similar REE patterns unlike the PCA biplot using Aitchison's logratio distances.

We have addressed the original concerns of reviewer 1 to our best knowledge and we are very sorry for the previous confusion. We hope we have clarified these points.

Geochemical discrimination and petrogenetic affinities of dykes intruding the Ladakh batholith, NW India

A.R. Heri[1,2,*], J. Bahl[3], I.M. Villa[4,5]

1 - University of Houston, Department of Earth and Atmospheric Sciences, 3507 Cullen Blvd, Houston, TX 77004, USA
2 - The University of Hong Kong, Department of Earth Sciences, Pokfulam Road, Hong Kong, China
3 - University of Texas, Health Science Center at Houston, Department of Epidemiology, 1200 Pressler Street, Houston, TX 77030, USA
4 - Università di Milano-Bicocca, Centro Universitario Datazioni e Archeometria, P. della Scienza 4, 20126 Milano, Italy
5 - Universität Bern, Institut für Geologie, Baltzerstr. 1+3, 3012 Bern, Switzerland

*Correspondence: (heri.alexandra@gmail.com)

Abbreviated title: Geochemical discrimination of Ladakh dykes

Eocene dykes extending over 50 km along the southern margin of the Ladakh batholith (NW India) fall into two main groups showing different orientation as well as isotope and trace element geochemistry. Both dyke families formed in the same tectonic setting over a time span of approximately 4 Ma. However, each family is far from monolithic, and therefore we tested several statistical approaches to identify geochemical subgroups from REE data and relate them to magmatogenetic processes.

Hierarchical Clustering and Multidimensional Scaling calculate similarities/dissimilarities among individuals of a population. Both statistical tools, when applied to the Ladakh dykes, reflect the east-west dichotomy. However, detailed quantification of the resulting grouping varies according to input data. Normalization to chondrites yields slightly different groupings from unnormalized concentration data. Population-internal REE normalization provides the most accurate grouping as revealed by the fact that multiple samples from the same dyke are assigned the closest relatedness. Independently from normalization, east-west dichotomy is mirrored by marked differences in degree of crustal assimilation and magma evolution, pointing to km-scale geological heterogeneity. Finally, dykes intruding the Ladakh batholith 150 km SE of the present samples are geochemically similar, but cluster as distinct group.

Key Words: relatedness of magmas, Ladakh batholith dykes

The Ladakh batholith has been intruded by dykes that differ chemically from the host rock, a common characteristic of plutonic complexes. The existence of such dykes along the southern margin of the Ladakh batholith was reported in the recent literature (Ahmad et al. 1998; Weinberg and Dunlap 2000; Ravikant and Guha 2002; Heri et al. 2015).

Weinberg and Dunlap (2000) described an andesitic dyke swarm between the villages Phyang and Taru 10 km west of Leh. Including these, Heri et al. (2015) reported almost 30 dykes in an area extending over 40 km west of Leh as far as Hemis Shugpachan, and suggested that more dykes can be found further west. Similarly, Ahmad et al. (1998) reported dykes near Nyoma, approximately 150 km southeast of Leh demonstrating that additional dykes occur in the eastern part of the batholith

The intrusion age of the dykes west of Leh was determined to be Eocene (Weinberg and Dunlap 2000; Heri et al. 2015). The dykes show variable compositions and degrees of differentiation, and their Sr-Nd isotopic variations cover a range larger than observed for the entire 30 000 km^2 Roman Volcanic Province (Hawkesworth and Vollmer 1979). Their heterogeneity is accompanied by a dichotomy in orientation and mineral assemblage. A structural separation of the dykes into a western, N-S to NW-SE trending group, and an eastern, E-W to NE-SW oriented group can be observed (Heri et al. 2015, p. 113, fig. 2). The change in dyke orientation is observed near Tunglung, which is located few kilometers upstream of Basgo, a village at the foot of the Ladakh batholith. Sr-Nd isotope systematics reveal affinity of the western group to mantle melts, whereas the eastern group shows a crustal isotope signature that is likely the result of crustal assimilation.

However, no trace element data on these dykes have been published. It is therefore unknown if and how variations observed in isotope geochemistry and major element composition are reflected in trace element geochemistry, in particular the division of the dykes into two groups located east and west of Tunglung. Further, it is unclear if these dykes are geochemically similar to the dykes east of Leh (Ahmad et al. 1998) and how they compare to other igneous bodies in the Himalaya-Karakorum-Tibet region.

Geological background

21 samples were collected from dykes intruding the Ladakh batholith. Detailed information on geochronology and isotope geochemistry as well as field

descriptions and petrography are presented in Heri et al. (2015), and briefly summarised here.

Samples were taken along the southern margin of the batholith just north of the Indus Suture over a distance of ca. 40 km west of Taru (cf. p. 113, fig. 1 and Supplementary Table A1 for coordinates of sampling locations in Heri et al. 2015). To assess effects of alteration on the geochemistry of the dykes, two dykes were sampled multiple times along strike. Each sample was given a sample identifier consisting of an acronym for sampling location (villages), dyke (number or letter) and sample number of the dyke, i.e. TuM1 is the sample taken from dyke M close to village Tunglung. Dykes in a given location are parallel, so no cross-cutting relationships were observed in the field.

The dykes are aphanitic to fine-grained, porphyritic with phenocrysts between 1 and 5 mm. Phenocryst mode ranges from <5 vol.% to approximately 70 vol.%. Plagioclase is predominant; hornblende and biotite are minor phenocryst phases. Some dykes east of Tunglung contain rounded and embayed quartz phenocrysts with and without cryptocrystalline coronas interpreted as reacted and partially resorbed xenocrysts. No such xenocrysts were found in dykes west of Tunglung.

Major element compositions reveal large variations in geochemistry (Heri et al. 2015). Most dykes are intermediate, but compositions range from basaltic (dyke 3) to rhyolithic (dyke N). In the total alkali vs silica (TAS) diagram (LeBas et al. 1986), most of the dykes scatter over the fields of andesite, trachyandesite, dacite and trachydacite (Heri et al. 2015, fig. 5). Considering K_2O contents of 2–6 wt.%, the dykes can be classified as high-K alkaline and shoshonitic arc rocks (Peccerillo and Taylor, 1976).

The dykes exhibit various degrees of alteration with secondary minerals being chlorite, calcite, sericite, epidote, and less abundant allanite and hematite. Although some dykes contain fresh phenocrysts, the majority of the dykes' phenocrysts are partially or entirely replaced by secondary minerals. In particular pseudomorphosis of chlorite after hornblende is common. A difference in secondary mineral abundance between the two groups of dykes has been observed. Epidote and clinozoisite modes are higher in dykes west of Tunglung, whereas calcite is predominant in the eastern dykes. Plagioclase phenocrysts are sericitised and/or altered to calcite, in some samples saussuritisation is observed.

Due to alteration and lack of pristine K-bearing mineral phases, only dyke 3, dyke M, and the two dykes U and V (samples ChU1 and ChV1, respectively) were dated by ^{39}Ar–^{40}Ar. Results showed that the dykes formed during the Early Eocene, with amphibole crystallization ages of 50 and 54 Ma (details given in Heri et al. 2015).

Dichotomy of the dykes is also observed in Sr-Nd isotopic composition; $\varepsilon_0(Nd)$ and $\varepsilon_0(Sr)$ values are mantle-influenced in the west of the field area. In the east, they are crust-dominated. There is substantial overlap with magmatic rocks of varying ages from different locations in the Himalaya-Karakorum-Tibet region (cf. Heri et al. 2015, p. 119, fig. 11b). $^{143}Nd/^{144}Nd$ and $^{87}Sr/^{86}Sr$ ratios show a large range given the spatial proximity of the dykes and the short time span during which they formed. Nd model ages (t_{DM}), which are expected to be the same for a suite of dykes, scatter over almost 1 Ga (cf. Heri et al. 2015, p. 119, fig 11c). These observations are attributed to varying degrees of crustal assimilation. The dykes west of Tunglung show mantle-like isotope signatures with small variation in t_{DM}, whereas the isotope composition of the dykes east of Tunglung, where xenocrysts were found, show crustal influence and large variation in t_{DM}.

Geochemical Characterisation

Trace element concentrations were determined by Activation Laboratories Ltd (Ontario, Canada) using sodium peroxide fusion and plasma mass spectrometry (FUS-ICP). Results are given in Table 1.

In any geological material, compositional variations can be due to one or more of the following causes: limited analytical repeatability of the concentration measurements, mineralogical inhomogeneity among hand specimens of the same rock, and alteration. In order to separate true variations from inherent noise, dyke 3 was sampled on three different locations along strike. Dyke 3 samples are given in blue diamond symbols in the following figures. Figure 1a shows a common-denominator diagram of the ratios of three Group 4 elements, Ti (Period 4), Zr (Period 5), and Hf (Period 6). As these elements are normally considered extremely immobile, at least to first order we can rule out alteration as a significant cause of spread observed for dyke 3 samples. Hf/Zr ratios of the three hand specimens deviate from the mean by 8 %. As Zr and Hf are both mainly hosted by zircon, we can conclude

that if the magmatic zircon grains of the dyke were homogeneous, the scatter would reflect the compound measurement uncertainty of the Hf/Zr ratio. However, Ti/Zr ratios deviate 14 % from the mean and as Ti and Zr are both more abundant than Hf, and thus expected to have a lower analytical uncertainty, it is most plausible that the variation in excess of the ca. 8 % analytical uncertainty is due to the variable mineralogical composition of the hand specimens, i.e. the mass ratio of the Ti-bearing phases (rutile ± titanite ± ilmenite ± biotite) to zircon. Figure 1b shows two further ratios of HFS elements: the Zr/Y ratio as a function of (La/Yb)N, i.e. La/Yb normalised to primitive mantle (Sun & McDonough, 1989). The Zr/Y ratio depends on the mass ratio of zircon to garnet, as garnet sequesters Yb and Y. If garnet remains in the residuum, the ascending melt is concomitantly depleted in Y and Yb. The three aliquots of dyke 3 plot closely together at the lower left of the diagram. The other dykes suggest an overall trend with a positive slope, which can be ascribed to residual garnet. A diagram displaying the role of garnet is shown in Fig. 1c: if only residual garnet were responsible for the positive trend in Fig. 1c, a negative correlation between Y/Al and $(La/Yb)_N$ would be observed. Neither the overall distribution nor the individual groups are compatible with a simple, single REE+Y partition mechanism.

To further investigate the geochemical homogeneity of dykes, multielement patterns of dyke 3 are plotted in Fig. 2a together with the samples of dykes U, V, 4 and 4a. Dyke 4a was found next to dyke 4 and believed to be an offshoot of the latter. Dykes U and V (samples ChU1 and ChV1) were found close to Hemis Shugpachan, the village furthest west in the field area. The dykes run parallel NW-SE at a distance of approximately 100 m, and are suspected to be comagmatic. Comparing these selected samples in Fig. 2a leads to two important findings. First, despite the alteration the dykes experienced, HFSE and REE remained immobile. Therefore, at least to first order, we can rule out alteration as a significant cause of any observed spread in REE patterns. In contrast, highly mobile elements such as Cs, Rb and Ba were affected and show considerable variations within dykes. This means REE and HFSE can be used as reliable parameters for geochemical inference, whereas LILE are less suitable. As a result, diagrams involving Rb such as tectonic discrimination diagrams after Pearce et al. (1984) will not yield accurate classifications. Second, Fig. 2a demonstrates the uniqueness of dyke magmas. Each has its own geochemical fingerprint discriminating it from all the other melts. It becomes obvious that samples

Ta4a1 and Ta042 are from the same dyke, whereas sample Ta041 originates from a different batch of magma. This was not recognized earlier due to partial coverage of the outcrop in the field and the similar, very fine-grained texture of the rock. Only the geochemical analyses finally revealed the fallacy. In the case of dykes U and V, the situation is more ambiguous. The two dykes crop out as parallel running individuals without apparent connection in the field. Dyke U consists of approximately 70 vol.% phenocrysts whereas dyke V exhibits <40 vol.%. Both dykes contain secondary minerals characteristic for greenschist metamorphic facies (Al-rich epidote, clinozoisite and chlorite) pointing towards involvement of fluids at temperatures exceeding 300 °C. However, secondary mineral mode is higher and the retrogression of primary magmatic minerals further advanced in dyke U compared to dyke V. From these observations, the two dykes could be interpreted as two individual magmatic bodies. However, Fig. 2a reveals that dykes U and V show virtually identical HFSE and REE patterns. The only notable difference is the slightly higher depletion in HREE, Ti and Y in dyke V compared to dyke U. Furthermore, ^{39}Ar–^{40}Ar stepwise heating has yield identical amphibole crystallization ages of 50.7 ± 0.3 (Heri et al. 2015). So there is ample evidence that although the dykes exhibit clear differences in primary and secondary features, they are likely to have formed from the same source at the same time.

Multi-element patterns of all sampled dykes are shown in Fig. 2b – for multiply sampled dykes only one pattern is given. The dykes are listed in spatial order from the most eastern dyke 1 (sample Ta011) to the most western dyke V (ChV1). They show large variations in concentrations exceeding one order of magnitude for Th, U, Nb, Ta and Pb, and strong depletion in Nb and Ta characteristic for arc rocks, whereas Ti anomalies associated with Nb and Ta depletion are less marked. Dykes plotted in quadrangular symbols are located east, and those in green, triangular symbols west of Tunglung. It becomes apparent that the dichotomy previously observed is also visible in trace element compositions. Dykes east of Tunglung are generally more enriched in trace elements than dykes west of Tunglung compared to primitive mantle.

Comprehensive geochemical data of dykes intruding the Ladakh batholith are sparse. One of the largest sets of major and trace element data was produced by Ahmad et al. (1998). These dykes are located approximately 150 km southeast of Leh

between Nyoma and Dungti, however exact locations of sampling sites were not provided. The petrographic descriptions suggest that they are (trachy) andesites/dacites similar to the dykes presented here. However, Ahmad et al. (1998) did not obtain radiometric ages and hence it is unknown whether all these dykes are contemporaneous or not. Fig. 2c shows the five dykes investigated by Ahmad et al. (1998) compared to the dykes of this study, for which only minimum and maximum values are given for better visibility. For two of the Nyoma dykes, multi-element patterns are given in dashed lines, because no REE concentrations were reported. The three dykes with known REE concentrations exhibit almost identical multi-element patterns. If only these samples are considered, the Nyoma dykes appear to be chemically more homogeneous than the ones west of Leh. However, if the two dyke samples without REE values are taken into account, more variation in chemical composition can be observed. Sample KH1M exhibits significantly different Ba, Th, Nb, P and Zr concentrations compared to the other Nyoma dykes. It would be beneficial to have REE concentrations of all dykes to better assess the extent of chemical variation, since geochemical heterogeneity is an important feature of dykes west of Leh. From the data presented by Ahmad et al. (1998), it is reasonable to assume that the Nyoma dykes are as variable in chemical composition as the dykes of this study. Enrichment of immobile elements and LREE of the Nyoma dykes is similar to the least enriched dykes of this study, whereas enrichment of HREE is similar to the most enriched ones (Fig. 2c). The comparison of multi-element patterns from multiply sampled dykes revealed that REE and HFSE were not affected by alteration and their behavior therefore reflects primary processes.

Due to the lanthanide contraction (Goldschmidt et al. 1925), a term describing the greater-than-expected decrease in ionic radii observed for the lanthanides, REE are of particular value relative to other immobile trace elements. REE concentrations normalized to primitive mantle values (Sun and McDonough 1989) are presented in Fig. 3a. For a better overview, only one sample per dyke is shown for multiply sampled dykes. Symbols are the same as in Fig. 2b. The dykes exhibit prominent enrichment in LREE with La and Ce concentrations up to several hundred times higher than primitive mantle. The dykes in the east are more highly enriched in LREE than the dykes in the west. Enrichment factors of HREE are an order of magnitude lower. The slightly stronger enrichment of Lu compared to Yb indicates amphibole in the source rock. The slope in REE is therefore better reflected by $(La/Yb)_N$ than

$(La/Lu)_N$. $(La/Yb)_N$ ranges from 11.2 (LiN1, dyke N) to 72.9 (UmH1, dyke H). The large difference in enrichment between LREE and HREE is evidence for very low degrees of melting (< 1 to 2 %).

Comparing the dykes of this study to the Nyoma dykes (Ahmad et al. 1998) further increases complexity. Fig. 3b shows the three Nyoma dykes, for which REE concentrations were reported, compared to the range in REE observed for the dykes of this study. The Nyoma dykes show less LREE enrichment and flatter REE slopes. However, REE concentrations are similar to the dykes east of Leh with LREE concentrations at the lower and HREE concentrations at the higher end of the observed spectrum. Multi-element patterns (Fig. 2c) suggest more variability in chemical composition than visible in Fig. 3b.

In essence, the same problem is encountered repeatedly - there is neither convincing similarity nor dissimilarity between the dykes east and west of Leh. The dykes west of Tunglung seem to be more similar to the Nyoma dykes east of Leh, although these are further away than the dykes east of Tunglung. The same is true for the distinction of the dykes west of Leh into two subgroups. Whereas LREE and LILE enrichment are clearly more pronounced in the dykes east of Tunglung, HREE concentrations of the two groups are overlapping. So ultimately, the question is: which ones of all these dykes are the most similar and how many groups can be distinguished? Based on primitive mantle-normalised multi-element and REE variation diagrams, no satisfactory answer can be found.

Haskin's approach

An alternative, but rarely employed strategy to handle geochemical data was suggested by Haskin (1990). Haskin pointed out that the normalisation of trace element data to undifferentiated reservoirs (i.e. chondrites, primitive mantle, MORB, *etc*.) is advantageous (elimination of Oddo-Harkins rule, comparability), but easily obscures subtle but potentially important differences amongst a set of related rocks. This is because the difference in geochemical composition between evolved rocks and primitive mantle is much higher than between evolved rocks and a reference sample that has undergone differentiation itself. Haskin (1990) recommended normalising samples to either their average or the petrologically most primitive sample of the set in order to enhance small differences amongst them. A similar procedure was applied to the dykes of this study by using dyke 7 (Ta071) as a normalising reference. Dyke 7

276 was chosen because its REE pattern was in the middle of the observed range
277 compared with all other samples. Figure 4a presents the REE concentrations of all
278 dyke samples (symbols are the same as in Fig. 2b) normalised to sample Ta071
279 (REE_{dyke7}). All dykes with positive REE slopes (HREE enriched compared to dyke 7)
280 are shown in Fig. 4b. Two groups of patterns are distinguishable. Group 1 is
281 comprised of the three samples from dyke 3 (Ta031, Ta032, Ta033). These samples
282 are virtually identical and act as an internal control for our analyses. Group 2
283 comprises all six dykes west of Tunglung, i.e. those that trend N-S to NE-SW. Five of
284 them show similar REE slopes and HREE concentrations. Only dyke N (sample
285 LiN1) exhibits a much steeper HREE slope with Lu enrichment being almost twice
286 that of the other dykes of group 2. In contrast, LREE concentrations are similar for all
287 six dykes, but could be ordered into two putative subgroups: one with $LREE_{dyke7}$ of
288 approximately 0.5 (dykes U, V, and N), and one with $LREE_{dyke7}$ between 0.75 and 1
289 (dykes M, Q, and R).
290 All dykes with negative or flat REE_{dyke7} slopes were assigned to group 3 and
291 are presented in Fig. 4c. The two types of REE patterns were grouped together, since
292 most of the generally flat REE patterns exhibit slightly negative slopes. All dykes east
293 of Tunglung belong to this group 3 except dyke 3 (group 1). Sample Ta041 has
294 normalized REE values close to 1.0, and thus is the sample most similar to reference
295 dyke 7. The dykes of group 3 show much more variation in REE patterns than
296 observed for groups 1 and 2. Based on slope and enrichment in REE, two subgroups
297 can be discerned. Group 3a comprises all those dykes with relatively flat REE patterns
298 ($(La/Lu)_{dyke7} < 1.4$) and $LREE_{dyke7}$ concentrations between 0.5 and 1.8. Group 3b
299 (dykes 5a, H and J) comprises the dykes with the strongest LREE enrichment of all
300 dykes. Further, group 3b dykes show peculiar REE patterns formed by LREE
301 concentrations increasing from La to Pr or Nd followed by a steep decrease in Sm,
302 Eu, Gd. $(La/Lu)_{dyke7}$ ratios for group 3b range from 1.59 (Ta5a1) to 2.36 (UmJ1). The
303 division of group 3 into two subgroups is straightforward except for two dykes. Dyke
304 1 (Ta011) exhibits high REE concentrations with LREE being similar to the dykes of
305 group 3b, however its REE concentrations smoothly decrease with $(La/Lu)_{dyke7} = 1.44$,
306 similar to the REE slopes of dykes belonging to group 3a. Therefore, dyke 1 was
307 attributed to group 3a instead of 3b, although there is similarity to the dykes of group
308 3b. Similarly, dyke I (sample UmI1) was ascribed to group 3a comprising dykes with
309 flat REE patterns, although dyke I is the only dyke of group 3 with a slightly positive

310 REE slope ($(La/Lu)_N = 0.87$) and could therefore be assigned to the dykes of groups 1
311 and 2. However, all those dykes show much steeper REE slopes.
312 The normalisation following Haskin (1990) demonstrates that the dykes can be
313 divided into several groups with distinct REE patterns. These different groups are
314 difficult to discern in conventional, primitive mantle normalised element variation
315 diagrams. However, the partitioning is not entirely unambiguous, as some samples
316 show REE patterns with characteristics attributable to more than one group. A further
317 step therefore requires independent evidence of the grouping of the dykes, as robust as
318 possible, in order to highlight systematics in the geochemical data that can be linked
319 to the dykes' petrogenesis.
320
321 **Hierarchical Clustering and Multidimensional Scaling**
322 The division of the Ladakh dykes into different groups as proposed above was
323 based on simple visual criteria distinguishing REE_{dyke7} patterns. The grouping is *ad*
324 *hoc*, since the visual criteria applied to delimit groups are arbitrary (albeit "rational").
325 Therefore, some of the samples match criteria defining more than one group, or none
326 at all. This also leads to artificially small groups (group 1, all samples from a single
327 dyke), or overly heterogeneous groups (group 3, smaller subgroups may be justified
328 based on REE slopes). In order to remove subjective selection criteria, it would be
329 desirable to have objective means to investigate the geochemical similarity and
330 dissimilarity of a set of samples. Quantitative methods have been developed to
331 determine natural groupings based on (dis)similarity among specimens. A widely
332 used approach is the application of the complementary statistical tools Hierarchical
333 Clustering (HC) and Multidimensional Scaling (MDS). Here we use these methods to
334 reduce the noise present in high dimensional data and assess the robustness of these
335 proposed groupings. Based on the descriptive analysis above, our expectation is that
336 the samples of dyke 3 (Ta031, Ta032, Ta033) will cluster together.
337 Hierarchical Clustering (Wessa 2012) is a statistical method, which calculates
338 the pairwise distance between variables to populate a distance matrix. The results of
339 HC are often presented as dendrograms such as the one presented in Fig. 5a. The
340 order of the samples, i.e. leaves of the dendrogram is irrelevant and can be rearranged
341 from left to right without changing the hierarchy, which is defined by the nodes. The
342 "height" is a measure for change, i.e. difference between samples – the shorter the
343 height, the more similar the samples. These dendrograms are produced following two

different strategies; top to bottom named “divisive” and bottom to top called “agglomerative”. For the dykes of this study, the divisive strategy was chosen, because it more naturally reflects the geologically reasonable assumption that the dykes formed from one progenitor magma above a subduction zone, which subsequently further diversified on its way towards earth’s surface through various interactions with the crust. This means, the dendrogram is constructed from the leaves towards to the root. The linkage criterion determines the distance between the clusters as a function of the pairwise distance. Complete-linkage clustering was chosen for the present dyke data. Further details on the different methods can be found in Kaufmann and Rousseeuw (1990).

A complementary method to HC is MDS, which visualizes similarity between individuals in relation to all others of a group (Clarke 1993). Similarity is expressed as distance between individuals in 2-dimensional or 3-dimensional Euclidean space. This distance is described by a data matrix of n dimensions in a single test, produced by k pairwise comparisons ($k = n(n-1)/2$) of n measured variables (e.g. REE concentrations). Distances between samples are arranged in a parsimonious manner, i.e. the algorithm looks for the simplest way to arrange data so that distances between samples are the smallest (Clarke and Gorley 2006). The population of dykes is visualized as dots in a 2-dimensional Euclidian space where similar sample profiles occupy similar positions, i.e. samples that plot close together in MDS are similar. In such a diagram, the similarity of samples to each other can be visualized based on as many parameters as desired independently from each other. The two methods are complementary and allow exploratory analysis of high dimensional data.

Results of HC and MDS of the dykes’ REE concentrations normalised to dyke 7 are presented in Fig. 5. HC (Fig. 5a) in principle supports the grouping of the dykes based on REE_{dyke7} patterns. However, one dyke of group 2 is assigned to group 3a, and one dyke from group 3a to group 3b. Group 3a is further split into two subgroups; one more similar to the dykes of group 2, and another one more similar to group 1. The dykes of group 3b are clustered together and singled out as the most different from all the other dykes. Figure 5b shows the 2D-projection of the n-dimensional space (n = REE = 14) generated by MDS. The samples of group 1, group 2, and group 3b cluster as individual groups. Group 3a however is not well defined and some of its members could be attributed to other groups.

HC and MDS demonstrate the merit of Haskin's (1990) suggestion to carefully choose the reference for normalising element concentrations. Fig. 6a shows HC and MDS of the Ladakh dykes if REE concentrations are normalised to primitive mantle (Sun and McDonough 1989) instead of dyke 7. Comparing Fig. 6a with Fig. 5 reveals that a change of normalisation reference affects the grouping of the dykes. No change relative to the dyke-7-normalised concentrations is recorded for the clustering of group 3b plus sample Ta011 and their distinction from the rest of the dykes. However, all other groupings are modified. Importantly, our internal control (group 1) no longer forms a distinct cluster and the distance between samples is increased. MDS shows that data fall into three groups with one large group of tightly clustered samples. Similarities in values of coordinate 1 are decisive for the grouping, since data spread in dimension 1 is much larger than dimension 2. Furthermore, the Euclidean Space generated by normalisation to primitive mantle is much larger than by normalisation to dyke 7. The data points spread over 200 units along coordinate 1 and 30 units along coordinate 2 compared to 5 and 3.5 units respectively. This is because normalising REE concentrations of dykes to primitive mantle results in considerably larger number values compared to normalisation to one of the dykes. To further investigtate the influence of normalisation reference on the grouping of the dykes, the same statistical analyses were performed using unnormalised REE values (ie. ppm). Figure 6c reveals that no difference in outcomes can be observed between using primitive mantle normalised and absolute REE concentrations. The clustering in the Euclidean space is identical, despite an increase along coordinate 1 by approximately 30 units. Just one difference in hierarchy can be observed for dyke Q (YaQ1), which is attributed to dyke 1 and one of the samples of dyke 3 instead of dykes 4 and 7. However, this does not affect the grouping of the dykes.

Normalisation to dyke 7 results in grouping that is different from normalisation using primitive mantle. However, groupings based on REE_{dyke7} are ultimately more accurate, since the recovery of group 1 (Ta031, Ta032, Ta033) reflects the field-based knowledge that these samples are from the same dyke 3. These samples are the most similar to each other, but only cluster together if the data is normalised to dyke 7, following Haskin's suggestion of population-internal normalisation. Nevertheless, some of the grouping is independent from the choice of normalisation reference. Samples TaX (dyke X), Ta021 (dyke 2), Ta4a1 and Ta042 (both dyke 4a) from Taru always cluster together. Similarly, dyke 1 (sample Ta011)

clusters with dykes 5a, H, and J (samples Ta5a1, UmH1, UmJ1), comprising group 3b. Dyke 1 is never grouped with dyke 4, which shows less enriched REE concentrations, but greater similarity of REE pattern (Fig. 4). These observations demonstrate that the HC and MDS of normalised or absolute REE concentrations group the dykes based on similarity in concentration, i.e. enrichment/depletion of REE. However, similar enrichment in REE and therefore statistical similarity may not have geological, geochemical or petrogenetic meaning. Similarity of REE pattern *shapes*, but not *concentrations* could be explained by passive enrichment of REE by crystal fractionation of mineral phases that do not incorporate or fractionate REE. Since similarity in REE patterns is commonly taken as indicator for petrogenetic relatedness, distinguishing the dykes' REE patterns based on shape instead of similarities in enrichment is desirable. The shapes of REE patterns is approximated by the REE slopes, which can be expressed as $(La/Lu)_N$ or $(La/Yb)_N$. We therefore chose to compare REE/Yb ratios, i.e. $(La/Yb)_{dyke\ 7}$, $(Ce/Yb)_{dyke\ 7}$, $(Pr/Yb)_{dyke\ 7}$, *etc* ending with $(Tm/Yb)_{dyke7}$, because Fig. 3a suggests that REE slopes of the dykes are better approximated by La/Yb than La/Lu. Fig. 7 shows the result of HC and MDS using $(REE/Yb)_{dyke\ 7}$ ratios instead of $(REE)_{dyke\ 7}$ values. Dyke 1 is now attributed to the dykes of group 3a (which includes dyke 4) instead of the highly LREE-enriched dykes of group 3b (orange). Also, dyke R (YaR1) is grouped with the other "western" dykes from group 2. The analysis of REE/Yb_{dyke7} values produces the grouping of the dykes based on REE pattern *shapes* instead of similarities in enrichment/depletion of REE. It supports the grouping based on visual comparisons of REE_{dyke7} patterns (Fig. 4), however the statistical analysis demonstrates that while some dykes fall into pretty clear clusters of similar REE profiles (*eg* group 2), other dykes mainly share the attribute of being very different to the other dykes (e.g. dykes of group 3b). The previously observed east-west dichotomy is not reflected in REE compositions of the dykes, i.e. the dykes cannot be reduced to two groups based on REE geochemistry.

One major difference between using $REE_{dyke\ 7}$ (Fig. 5) and $(REE/Yb)_{dyke\ 7}$ (Fig. 7) for statistical analysis is visualised by MDS. Whereas the range of data points (approximately 5 units) in dimension 1 (coordinate 1) does not change, the data distribution in dimension 2 (coordinate 2) is reduced from approximately 4 units (Fig. 5b) to less than 1 (Fig. 7b). The same is discernible from HC: the branches of the dendrogram in Fig. 7a are longer towards the root and shorter towards the leaves compared to the dendrogram in Fig. 5a. In other words, the comparison of REE slopes

445 rather than REE enrichment/depletion to a reference material reduces the variation in
446 one dimension of the 2D-Eucledian space, i.e. the $(REE/Yb)_N$ *values* are more similar
447 to each other than the $(REE)_N$ *values*.
448 Since the grouping of the dykes based on REE is affected by changing
449 normalisation reference, the effect of normalisation on REE/Yb was investigated.
450 Figure 8a shows the results from HC and MDS of REE/Yb normalised to primitive
451 mantle and Fig. 8b of unnormalised REE/Yb ratios. All dykes are attributed to the
452 groups originally defined based on REE pattern shape (Fig. 4, Fig. 7). Only the
453 hierarchy within individual groups is slightly changed compared to Fig. 7a.
454 Analogously to the experiments with REE, the 2D-Euclidean space becomes
455 progressively larger from dyke-7-normalised (Fig. 7) to primitive mantle-normalised
456 to unnormalised REE/Yb concentrations (Fig. 8).
457 The statistical analysis of compositional data is complicated by two main
458 problems: the constant-sum constraint and the marked curvature that such data sets
459 often exhibit (Aitchison 1983). The constant-sum constraint describes the requirement
460 that the components of each vector in the multidimensional space (i.e. positive
461 simplex) must add up to unity. This is the case for major elements, since major
462 element oxides account for almost 100% of the rock's composition. It is suggested by
463 Aitchison (1982, 1983) to proceed analogously with subcompositions, and normalise
464 the data to one. This approach has been applied to different selections of trace
465 elements (eg. Vermeesch, 2015), ie trace elements are expressed in relative
466 abundances summing up to one. In this study, we present another approach to
467 comparing rock samples based on the commonly used REE/multi-element variation
468 diagram. In REE/multi-element variation diagrams, not relative abundances of REE
469 and other trace elements are compared, but the enrichment/depletion of these elements
470 in relation to a reference material, for example chondrite or primitive mantle. As a
471 consequence, these values are never expected to sum up to unity. It is debatable
472 whether comparing samples' trace element composition based on relative abundances
473 or enrichment/depletion factors is more informative. One advantage of choosing
474 enrichment/depletion factors over relative abundances is the preservation of
475 information about the total abundance of the elements in question. If element
476 concentrations are normalised to one, this information is lost. Curvature in data is not
477 only observed within the simplex, and therefore our data set potentially suffers from
478 curvature as well. A solution to both these problems, curvature and constant-sum

constraint, is the use of the non-linear, logarithmic function (Aitchison 1982, Aitchison 1983). To test our approach for problems arising from the potential of curvature in the data and the constant-sum constraint, we re-analysed all data after logarithmic transformation. As it can be seen from Fig. 9, the results from HC and MDS are indistinguishable indicating that both issues are no relevant to this data set.

Comparisons with Literature Data

HC and MDS provide means to rapidly identify the most similar samples out of any number of samples and therefore well suited for comparisons of data sets from different studies. Questions such as "how similar are the dykes of this study to the dykes 150 km SE of Leh (Ahmad et al. 1998)?" can be answered quantitatively based on statistical grounds rather than visual impression from REE/multi-element variation diagrams.

For reasons detailed above, dyke 7-normalised REE/Yb ratios (except Lu/Yb) were chosen to compare the dykes of this study with the Nyoma dykes (Ahmad et al., 1998). Since Pr, Tb, Ho and Tm were not reported for the latter, only $(La/Yb)_{dyke\ 7}$, $(Ce/Yb)_{dyke\ 7}$, $(Nd/Yb)_{dyke\ 7}$, $(Sm/Yb)_{dyke\ 7}$, $(Eu/Yb)_{dyke\ 7}$, $(Gd/Yb)_{dyke\ 7}$, $(Dy/Yb)_{dyke\ 7}$ and $(Er/Yb)_{dyke\ 7}$ were used for comparison. Figure 10 shows the results from HC and MDS with conventional REE diagrams given below the dendrogram to illustrate the grouping produced from HC. Colours correspond to the groups of dykes identified in the previous section. Hierarchical Clustering (Fig. 10a) demonstrates that the Nyoma dykes SE of Leh (red) are first of all most similar to each other. However, they do not form their own group such as the dykes of group 3b (orange) and 3a (black). They form a subgroup within the dyke family with positive $REE_{dyke\ 7}$ slopes comprising the dykes west of Tunglung (group 2 in green) and dyke 3 (blue). Multidimensional Scaling (Fig. 10b) exemplifies that the Nyoma dykes east of Leh are geochemically most closely related to dykes N, U and V.

The large range in trace element and isotope composition of the dykes of this study finds its counterpart in the similarly heterogeneous, post-collisional potassic magmas of the Tibetan plateau. HC and MDS are ideal tools to compare the dykes of this study with the comprehensive data set on Miocene post-collisional magmatism across the Tibetan plateau by Williams et al. (2004). It would be a highly time-consuming exercise to find the most similar REE patterns amongst all samples from this and their study (76 samples in total) using conventional element variation

513 diagrams. HC and MDS are capable of solving this task instantaneously and
514 statistically sound. As in the previous example, dyke 7-normalised REE/Yb ratios are
515 compared. Results from HC of the post-collisional magmas and the dykes of this
516 study are presented in Fig. 11 including REE variation diagrams analogous to the
517 previous example (Fig. 10a). Samples in the REE variation diagrams are listed in the
518 order they appear at the tips of the dendrogram from left to right. Post-collisional
519 samples from southern Tibet are coloured pink, whereas samples from northern Tibet
520 are given in bright blue. Samples with positive slopes compared to dyke 7 (y=1 in
521 panel three) are grouped together (first two panels), samples with nearly horizontal
522 patterns are grouped together (third panel) and those with negative slopes are grouped
523 together (last three panels). The dykes of this study do not cluster as one group
524 distinct from the post-collisional magmas, but are attributed to different groups of
525 post-collisional magmas. Only the three samples of dyke 3 still cluster as one group
526 validating the approach of using REE/Yb_{dyke7}. Some of the grouping persists, for
527 example many of the dykes of group 3a still cluster together. Remarkable are the
528 almost identical patterns observed in certain groups of post-collisional magmas. The
529 high similarity is particularly well recognisable in the Euclidean space shown in Fig.
530 12, where some samples form tighter clusters than the three samples from dyke 3. For
531 example, samples identified with K90 prefix form unexpectedly tight clusters (inset
532 Fig. 12). These samples were first published by Turner et al. (1996), and later
533 included in the publication by Williams et al. (2004). They originate from two
534 sampling locations labelled by the authors as VII and VIII, however some samples
535 were attributed to different sampling locations in the two publications and no
536 coordinates were reported. HC and MDS (Figs. 11 and 12) easily distinguish between
537 samples from Kunlun (26, 27, 29, 31, 32, 24, 28) and Dogai Coring, which cluster
538 together with dyke 4a (Ta4a1 and Ta042). Figure 12 illustrates that the Eocene dykes
539 of this study are similar in REE composition to post-collisional magmas from
540 northern and southern Tibet. The Eocene Ladakh dykes are dispersed within the
541 Euclidean space occupied by Miocene post-collisional magmas with certain Ladakh
542 dykes having very similar REE profiles to some post-collisional magmas (e.g. dykes 1
543 and 4a), whereas others show more exclusive REE compositions (e.g. dykes of group
544 3b).
545
546 **Isotopic Evidence**

Another approach used for tracing common origins of igneous rocks is fingerprinting by Nd-Sr isotopes. In this case isotope fingerprinting cannot provide strong evidence for or against relatedness of the dykes based on mantle extraction ages, since the observed Nd-Sr isotopic ratios are most likely controlled by the mass balance of crustal assimilation (Heri et al. 2015). Crustal assimilation includes processes such as high-T melting of fertile rocks, magma mixing, magmatic stoping and possibly involves fluids released from the subducting slab. Figure 13a reveals that crustal assimilation did not only affect isotope systems, but also trace element content of the dykes. REE slopes increase with increasing degree of crustal assimilation, i.e. increasing ε(Sr). The dyke samples fall onto two distinct regressions with different slopes. Since only four dykes contained dateable phenocrysts, arguments involving the ages of the dykes and the chronological order of events are not well supported. Nevertheless, three 50 Ma old dykes (dykes 3, U and V) all plot on the regression with the shallower slope, whereas the one 54 Ma dyke sample (TuM1) plots on the steep regression. The 54 Ma magmatic event records stronger LREE enrichment per ε(Sr) than the later, 50 Ma event. This is suggestive of different petrogenesis during the older (54 Ma) compared to the younger (50 Ma) magmatic episode. The two correlations are much less marked in $(La/Lu)_{dyke\ 7}$ vs. ε(Nd) shown in Fig. 13b, indicating that Nd isotopic compositions were less affected than Sr isotopic compositions during dyke formation. The implications from these observations are manifold. Since two magmatic events involving crustal assimilation were responsible for the formation of the dykes, similar dykes were produced in one area at different times. Dykes west of Tunglung show more pristine Nd and Sr isotopic ratios whereas dykes east of Tunglung have undergone higher degrees of crustal assimilation with dykes of group 3b (orange) being the most enriched samples. Differences in LREE composition within dykes of group 2 separating them into subgroups can be explained – dykes N, Q and R with higher LREE enrichment plot on the 54 Ma regression line, whereas dyke T, U and V with lower LREE enrichment plot on the 50 Ma regression line. By only comparing REE patterns, this petrogenetic link cannot be recognised.

Discussion

In this study, we concentrated on REEs, but there are no limits in terms of parameters that can be chosen for comparison given the proper treatment of the input

data. Supervision (including geological meta-knowledge) is required in interpreting outcomes as illustrated by two examples involving literature data. The Nyoma dykes in the first example (Ahmad et al. 1998) are geochemically similar to the dykes of this study and since all these dykes are located in the same tectonic setting along the southern margin of the Ladakh batholith, it is very likely that they all share the same genesis. However, the assessment of similarity is solely based on REEs of three Nyoma dykes. REE values for the other two sampled Nyoma dykes could potentially change the grouping of the dykes. Further, these dykes could theoretically be tens of Ma older or younger than the dykes of this study. Without radiometric age data, there is no absolute certainty – there is only geochemical similarity between the dykes SE of Leh and dykes of group 1 and 2 of this study.

It is clear that a large statistical distance implies a low degree of cogeneticity. However, the reverse is not true: statistical proximity is no guarantee of genetic relatedness. This point is well illustrated by the second example, where the dykes of this study were compared to magmas from across the Tibetan plateau. Based on the comparison of REE patterns, similarities are readily discernible even though these magmas are from a different part of the Himalaya-Karakoram-Tibet region and have formed $\geq$ 30 Ma later than the dykes of this study. Using HC and MDS to conclude that they belong to the same suite would be incorrect.

An additional issue are representativity and sampling bias. The importance of recognising the most similar samples is well demonstrated by the data set on Tibetan post-collisional magmas. Based on REE/Yb comparisons, HC and MDS identified two tight clusters corresponding to two sampling locations. As can be seen from the REE variation diagrams in Fig. 11, samples within one cluster show virtually identical REE patterns. The question arises if this high similarity is due to higher homogeneity of the sampled magma compared to dyke 3 from Ladakh, or if the similarity is due to sampling bias. It is not possible to infer from the publications how representative the samples are for the entire geologic body they came from. Exact sampling locations (GPS data) and/or detailed field maps/descriptions would be of great assistance in assessing sampling strategies and identifying possible sampling bias. This is important - group 1 in this study is representing only one dyke and is strictly spoken not “a group of dykes”. Bias is introduced by overrepresentation of multiply sampled dykes compared to the other dykes of the data set.

As can be seen from Fig. 1, the petrogenesis of the dykes is controlled by at least two superposed magma chamber processes. The process controlling the slopes of REE patterns is not identical to that controlling the absolute concentrations. REE concentrations depend on the degree of partial melting, differentiation, crustal assimilation and fractional crystallization, whereas the La/Yb ratio is affected by the modal abundance of garnet in the residuum and of apatite ± monazite ± xenotime in the dyke magma. In summary, the choice of a diagram to ascertain the relatedness of the dykes is equivalent to choosing whether the best way to quantify magmatogenesis is via mineralogy (apatite, monazite, garnet) or via differentiation and crustal assimilation. As these magmatogenetic processes always play the same role, it is not surprising that the two different classes of diagrams (concentrations or ratios) give a robust and reproducible grouping despite the apparently contrasting ways to normalize the REE concentration data (primitive mantle, dyke 7).

Conclusions and Implications

We have identified a great chemical diversity among dykes that intrude the Ladakh Batholith in a relatively small area West of Leh. This observation discourages the use of a single lump term, such as "Ladakh batholith dykes", to describe a varied set of magmatic episodes having multiple petrogeneses. Within this complex set of magmatic (and altered) rocks we have used REE to identify groups that differ in their genetic relatedness. Most samples can be assigned to groups in a robust fashion that does not depend on the choice of normalisation. A few samples, however, can shift groups according to the choice of reference sample. This highlights the fact that the human wish to reduce petrogenesis to one dominant magma chamber process can introduce an interpretive bias when several petrogenetic processes operate simultaneously with local differences. Furthermore, the orientation of the dykes is not related to their age but to local stress fields. No chronological information concerning regional stress fields can be inferred from these dykes at present.

As is the case for many other scientific disciplines, data collections in geochemistry have become so large that innovative approaches to compare newly generated sample sets with literature data are sought for. Statistical tools such as HC and MDS open new perspectives on interpretation of data. There are two main advantages of these tools, which were demonstrated in this study. First, they allow for the analyses of much more parameters simultaneously and therefore make for

statistically more reliable interpretations concerning similarity/dissimilarity of rocks. Second, comparisons of (several) hundred samples, i.e. amount of data difficult to handle by humans and common spreadsheets, become a matter of routine. Despite the potential ease for adoption of these tools, they should be used with careful supervision. Statistical correlations might not translate to meaningful geological inferences. Collections should include multiple samples collected from the same geological formation and used as a 'sanity check' and internal control. We argue that knowing the age and exact sampling locations of the compared rock samples is critical, since geochemically similar magmatic bodies can be produced in various places at different points in time.

Acknowledgements

Major and trace element analyses were funded by the Leibnitz Preis (awarded to Klaus Mezger). K. Mezger is thanked for the generous contribution. Xueting Qiu is thanked for help with statistical analyses. Jess King is thanked for financial and personal assistance in collecting the rock samples. The fieldwork in Ladakh was funded by The University of Hong Kong, Small Project Funding grant 200707176193 awarded to Jess King.

References

Ahmad, T., Thakur, V.C., Islam R., Khanna, P.P., Mukherjee, P.K., 1998. Geochemistry and geodynamic implications of magmatic rocks from the Trans-Himalayan arc. Geochemical Journal, 32: 383–404.

Aitchison, J., 1982. The Statistical Analysis of Compositional Data. Journal of the Royal Statistical Society, Series B (Methodological) 44: 139–177.

Aitchison, J., 1983. Principal component analysis of compositional data. Biometrika, 70: 57–65.

Clarke, K.R., 1993. Non-parametric multivariate analyses of changes in community structure. Australian Journal of Ecology, 18: 117–143.

680 Clarke, K.R., and Gorley, R.N., 2006. PRIMER v6: User Manual/Tutorial. PRIMER-
681 E, Plymouth.
682
683 Goldschmidt, V.M., Ulrich, F., Barth, T. 1925. Skrifter utg. av det Norske
684 Videnskaps-akademi i Oslo. I. Mat.-naturv. klasse, No. 5
685
686 Haskin, L.A., 1990. Presidential Address: PREEconceptions pREEvent pREEcise
687 predictions. Geochimica et Cosmochimica Acta, 54: 2353–2361.
688
689 Hawkesworth, C.J., Vollmer, R., 1979. Crustal contamination versus enriched mantle
690 - Nd-143-Nd-144 and Sr-87-Sr-86 evidence from the Italian Volcanics. Contributions
691 to Mineralogy and Petrology, 69: 151–165.
692
693 Heri, A.R., Aitchison, J.C., King, J.A., Villa, I.M., 2015. Geochronology and isotope
694 geochemistry of Eocene dykes intruding the Ladakh Batholith. Lithos, 212–215: 111–
695 121.
696
697 Kaufmann, L., and Rousseeuw, P.J., 1990. Finding Groups in Data: An Introduction
698 to Cluster Analysis. J. Wiley & Sons, New York, 368p.
699
700 LeBas, M.J., LeMaitre, R.W., Streckeisen, A., Zanettin, B., 1986. A chemical
701 classification of volcanic rocks based on the total alkali silica diagram. Journal of
702 Petrology, 27: 745–750.
703
704 Pearce, J.A., Harris, N.B.W., Tindle, A.G., 1984. Trace Element Discrimination
705 Diagrams for the Tectonic Interpretation of Granitic Rocks. Journal of Petrology, 25:
706 956–983.
707
708 Peccerillo, A. and Taylor, S.R., 1976. Geochemistry of Eocene calc-alkaline volcanic
709 rocks from the Kastamonu area, Northern Turkey. Contributions to Mineralogy and
710 Petrology, 58: 63–81.
711

712 Ravikant, V. and Guha, D., 2002. Ultrapotassic postcollisional dyke from the Leh
713 batholith, Northwest Himalaya. Journal of the Geological Society of India, 59: 473–
714 476.
715
716 Sun, S. and McDonough, W.F., 1989. Chemical and isotopic systematics of oceanic
717 basalts: implications for mantle composition and processes. Geological Society,
718 London, Special Publications, 42: 313–345.
719
720 Turner, S., Arnaud, N., Liu, J., Rogers, N., Hawkesworth, C., Harris, N., Kelley, S.,
721 Van Calsteren, P., Deng, W., 1996. Post-collision, Shoshonitic Volcanism on the
722 Tibetan Plateau: Implications for Convective Thinning of the Lithosphere and the
723 Source of Ocean Island Basalts. Journal of Petrology, 37: 45–71.
724
725 Vermeesch, P., and Garzanti, E., 2015. Making geological sense of 'Big Data' in
726 sedimentary provenance analysis. Chemical Geology, 409:20–27.
727
728 Weinberg, R.F., and Dunlap, W.J., 2000. Growth and Deformation of the Ladakh
729 Batholith, Northwest Himalayas: Implications for Timing of Continental Collision
730 and Origin of Calc-Alkaline Batholiths. The Journal of Geology, 108: 303–320.
731
732 Wessa, P., (2012). Hierarchical Clustering (v1.0.3) in Free Statistics Software
733 (v1.1.23-r7), Office for Research Development and Education, URL
734 http://www.wessa.net/rwasp_hierarchicalclustering.wasp/
735
736 Williams, H., Turner, S., Pearce, J., Kelley S., Harris N., 2004. Nature of the Source
737 Regions for Postcollisional, Potassic Magmatism in Southern and Northern Tibet
738 from Geochemical Variations and Inverse Trace Element Modelling. Journal of
739 Petrology, 45: 555-607.
740

741 **Figure captions**
742
743 **Fig. 1:** Trace element diagrams using HFSE and REE. Samples of dyke 3 are given in
744 blue diamonds. (**a**) Hf/Zr vs. Ti/Zr, (**b**) Zr/Y vs. $(La/Lu)_N$ and (**c**) $(La/Lu)_N$ vs. Y/Al.
745
746 **Fig. 2**: Multielement variation diagrams. (**a**) Samples of the same dyke and samples
747 from dykes suspected to be comagmatic. (**b**) All dykes and (**c**) range of variation

observed for the dykes of this study compared to Nyoma dykes SE of Leh (Ahmad et al., 1998).

Fig. 3: REE normalized to primitive mantle values (Sun and McDonough, 1989). (**a**) All dykes of this study and (**b**) range in REE concentrations compared to the Nyoma dykes (Ahmad et al., 1998).

Fig. 4: REE concentrations normalized to dyke 7 (sample Ta071). (a) All dykes of this study. Dykes east of Tunglung (E-W to NE-SW oriented) are shown as square symbols and colours of purple and red plus the three samples of dyke 3 in dark blue. The dykes west of Tunglung (N-S to NW-SE oriented) are given in green tones and triangular symbols. (**b**) Dykes with positive REE slopes and (**c**) dykes with negative REE slopes or flat REE patterns.

Fig. 5: REE concentrations of all dyke samples normalized to dyke 7. (**a**) Hierarchical Clustering and (**b**) Multidimensional Scaling.

Fig. 6: (a) Hierarchical Clustering and Multidimensional Scaling of REE concentrations of all dyke samples normalised to primitive mantle values (Sun and McDonough, 1989). (**b**) Hierarchical Clustering and Multidimensional Scaling of unnormalised REE concentrations (ppm).

Fig. 7: REE/Yb ratios normalised to dyke 7 (Ta071). (**a**) Hierarchical Clustering and (**b**) Multidimensional Scaling.

Fig. 8: Hierarchical Clustering and Multidimensional Scaling of REE/Yb ratios normalised to primitive mantle (Sun and McDonough, 1989) (**a**) and unnormalised REE/Yb ratios (**b**).

Fig. 9: Hierarchical Clustering and Multidimensional Scaling of (**a**) log(REE), (**b**) log(REE/Yb), (**c**) $\log((REE/Yb)_{dyke7})$.

Fig. 10: $(REE/Yb)_{dyke\ 7}$ of all dykes samples of this study compared to the Nyoma dykes (Ahmad et al., 1998). (**a**) Hierarchical Clustering; $(REE)_{dyke\ 7}$ variation diagrams are shown for illustration. Dykes are plotted according to groups identified by Hierarchical Clustering. (**b**) Multidimensional Scaling.

Fig. 11: Hierarchical Clustering of $(REE/Yb)_{dyke\ 7}$ of all dyke samples of this study and post-collisional magmas from northern and southern Tibet (Williams et al., 2004 and references therein).

Fig. 12: Multidimensional Scaling of $(REE/Yb)_{dyke\ 7}$ of all dykes of this study and postcollisional lavas from across the Tibetan plateau (Williams et al., 2004 and references therein).

Fig. 13: $(La/Yb)_{dyke\ 7}$ ratios of all dyke samples plotted against (**a**) Sr isotopic compositions and (**b**) Nd isotopic compositions, given in epsilon notation (Heri et al., 2015).

Table 1. *Trace element concentrations of all dyke samples. Major element concentrations*

				dyke 1	*dyke X*	*dyke 2*	*dyke 3*
Analyte	Unit	Detection Limit	Method	Ta011	TaX	Ta021	Ta031
Sc	ppm	1	FUS-ICP	10	9	10	19
Be	ppm	1	FUS-ICP	3	4	2	3
V	ppm	5	FUS-ICP	134	126	140	203
Cr	ppm	20	FUS-MS	bd	bd	200	90
Co	ppm	1	FUS-MS	18	13	14	27
Ni	ppm	20	FUS-MS	bd*	bd	bd	50
Cu	ppm	10	FUS-MS	20	60	50	70
Zn	ppm	30	FUS-MS	150	110	130	100
Ga	ppm	1	FUS-MS	24	20	19	19
Ge	ppm	0.5	FUS-MS	1.6	1.1	1.5	1.8
As	ppm	5	FUS-MS	7	bd	8	6
Rb	ppm	1	FUS-MS	68	154	41	95
Sr	ppm	2	FUS-ICP	1270	1149	721	768
Y	ppm	0.5	FUS-MS	18.7	11.4	13.3	19.3
Zr	ppm	1	FUS-MS	338	318	280	227
Nb	ppm	0.2	FUS-MS	15.7	18.4	13.6	38.8
Mo	ppm	2	FUS-MS	bd	bd	7	bd
Ag	ppm	0.5	FUS-MS	1.4	1.4	0.6	0.6
In	ppm	0.1	FUS-MS	bd	bd	bd	bd
Sn	ppm	1	FUS-MS	2	2	2	3
Sb	ppm	0.2	FUS-MS	0.4	0.5	bd	1.5
Cs	ppm	0.1	FUS-MS	2.3	6.3	3.8	4.4
Ba	ppm	3	FUS-ICP	1567	1350	413	989
La	ppm	0.05	FUS-MS	107	52.8	58.1	42.1
Ce	ppm	0.05	FUS-MS	213	111	119	81.3
Pr	ppm	0.01	FUS-MS	22.9	12.9	13.7	9.43
Nd	ppm	0.05	FUS-MS	83	49.2	49.2	35.5
Sm	ppm	0.01	FUS-MS	12.9	7.71	8.05	6.8
Eu	ppm	0.005	FUS-MS	2.93	1.9	2	1.86
Gd	ppm	0.01	FUS-MS	8.44	4.99	4.96	5.53
Tb	ppm	0.01	FUS-MS	0.92	0.56	0.61	0.79
Dy	ppm	0.01	FUS-MS	4	2.5	2.87	4.08
Ho	ppm	0.01	FUS-MS	0.64	0.43	0.49	0.74
Er	ppm	0.01	FUS-MS	1.76	1.12	1.27	1.93
Tm	ppm	0.005	FUS-MS	0.223	0.149	0.164	0.258
Yb	ppm	0.01	FUS-MS	1.35	0.9	1.01	1.67
Lu	ppm	0.002	FUS-MS	0.22	0.139	0.157	0.267

Hf	ppm	0.1	FUS-MS	5.3	5.8	5.1	4.4
Ta	ppm	0.01	FUS-MS	1.03	1.15	0.8	2.89
W	ppm	0.5	FUS-MS	bd	bd	bd	bd
Tl	ppm	0.05	FUS-MS	0.53	1.11	0.22	0.55
Pb	ppm	5	FUS-MS	33	18	16	61
Bi	ppm	0.1	FUS-MS	0.7	0.3	bd	0.7
Th	ppm	0.05	FUS-MS	26.7	13.9	9.65	17.3
U	ppm	0.01	FUS-MS	5.38	4.21	2.06	4.46

*bd = below detection

s can be found in Heri et al. 2015.

dyke 3	*dyke 3*	*dyke 4a*	*dyke 4*	*dyke 4a*	*dyke 5a*	*dyke 5*	*dyke 7*
Ta032	Ta033	Ta4a1	Ta041	Ta042	Ta5a1	Ta051	Ta071
26	23	10	7	10	11	5	8
3	3	3	3	3	14	6	3
236	207	124	97	121	106	57	97
190	170	250	610	470	70	bd	bd
33	33	16	13	17	14	6	13
70	70	bd	bd	20	60	bd	bd
70	70	90	60	50	90	30	30
110	120	130	140	130	100	80	90
18	19	22	23	23	22	19	21
1.9	1.6	1.5	1.5	1.6	2	1.8	1.4
bd	8	bd	bd	bd	11	7	6
143	107	62	84	63	332	172	97
777	752	1030	1097	1027	1158	640	869
19.7	18.9	13	9.5	13.3	14.1	6.7	10.2
196	222	288	292	282	405	175	247
34.1	36.7	14.1	13	12.9	15.4	9	15.9
2	3	9	24	17	4	bd	bd
bd	0.9	1.2	1.1	1.1	1.5	bd	1
bd	bd	bd	bd	bd	bd	bd	bd
3	2	2	2	2	7	4	2
1	0.9	0.5	0.4	0.5	0.7	1.1	0.4
15	9.7	5.3	5.3	6.5	15.5	18	4.3
875	963	1102	854	1190	2809	1127	957
36.8	35.4	75.1	44.4	77.7	89.3	39.3	43.9
73.8	70.5	144	91	150	199	73.1	89
8.86	8.09	15.1	9.72	15.8	24.5	7.79	9.6
34.6	32.2	53.4	36.1	56.9	99.5	26.7	35.6
6.95	6.26	8.16	5.81	8.7	16.5	4.19	5.9
1.91	1.81	2	1.48	2.09	2.61	0.939	1.51
5.74	5.41	5.52	3.92	5.81	8.3	2.37	4.21
0.79	0.75	0.61	0.44	0.64	0.77	0.3	0.48
4.13	3.88	2.73	2	2.77	3.11	1.4	2.18
0.75	0.69	0.46	0.34	0.46	0.52	0.24	0.37
1.89	1.89	1.23	0.93	1.29	1.39	0.62	0.99
0.257	0.249	0.166	0.124	0.164	0.177	0.084	0.13
1.59	1.58	0.99	0.76	0.99	1.04	0.58	0.8
0.251	0.251	0.161	0.124	0.163	0.166	0.096	0.13

4.1	4	4.8	4.9	4.8	7.8	4.2	4.4
2.37	2.49	0.77	0.74	0.85	1.31	1.42	0.98
bd	bd	bd	bd	bd	bd	bd	bd
0.82	0.67	0.44	0.53	0.49	3.55	1.51	0.7
43	28	65	25	27	247	116	36
0.8	0.4	0.4	0.2	0.2	6.5	3.1	0.6
13.9	13.8	16.9	9.81	18.4	132	31.6	14.2
3.3	3.37	3.33	3.71	3.58	19.5	10.6	4.63

dyke H	*dyke I*	*dyke J*	*dyke M*	*dyke N*	*dyke Q*	*dyke R*	*dyke U*
UmH1	UmI1	UmJ1	TuM1	LiN1	YaQ1	YaR1	ChU1
11	10	12	12	3	10	9	11
5	2	5	1	2	2	2	1
150	121	175	128	23	128	107	129
40	20	50	40	660	400	440	bd
18	15	19	15	2	20	8	16
30	bd	30	20	bd	bd	bd	bd
80	30	80	bd	40	bd	bd	40
100	130	100	80	60	40	40	110
22	21	21	24	15	24	18	18
1.6	1.4	1.9	bd	2.2	bd	1.8	1.6
bd	bd	9	bd	20	11	25	28
269	50	250	41	120	86	119	50
1139	863	1334	587	327	681	546	570
11.6	10.6	12.9	10.7	14.5	10.1	10.5	11.8
473	279	444	192	273	182	197	151
31.7	15.3	34.9	7.9	7.9	8.6	8.4	4
bd	bd	bd	bd	25	11	16	bd
1.9	1	1	bd	0.7	bd	bd	bd
bd	bd	bd	bd	bd	bd	bd	bd
5	1	5	bd	2	bd	2	16
0.7	0.3	1.1	bd	1.2	3.4	5.7	2.7
9.3	3.3	10	2.5	9.9	4.3	2.7	4.4
2412	667	2810	454	750	584	627	529
91.4	39.5	109	34.7	27.9	43.8	33	20.6
195	82.7	229	71.2	53.3	83.9	67.3	42.6
22.3	9.25	26.3	7.06	5.73	8.18	7.49	4.93
80.8	34.5	91.6	27	19.6	30.7	27.4	18.9
10.9	5.78	12	5.04	3.42	5.45	4.8	3.65
2.3	1.52	2.46	1.27	0.806	1.32	1.15	0.987
5.99	4.13	5.74	3.69	2.69	3.84	3.25	2.9
0.59	0.5	0.62	0.52	0.43	0.5	0.41	0.42
2.54	2.22	2.85	2.52	2.52	2.4	2.18	2.21
0.39	0.39	0.47	0.46	0.51	0.43	0.37	0.42
1.17	1.02	1.21	1.22	1.54	1.12	1.03	1.15
0.148	0.128	0.142	0.195	0.242	0.174	0.139	0.173
0.9	0.81	0.86	1.24	1.79	1.12	0.96	1.17
0.135	0.134	0.137	0.205	0.307	0.188	0.157	0.184

9	4.5	9.2	4.7	5.6	4.4	4.2	3.4
2.17	0.88	2.48	0.53	0.74	0.53	0.56	0.29
1.7	bd	2.5	bd	bd	1.5	1	bd
1.42	0.34	1.43	0.28	0.38	0.57	0.77	0.37
25	22	40	8	10	10	8	15
0.7	0.2	0.4	0.2	0.2	0.4	0.2	0.2
23.3	5.28	25.2	4.34	21.3	6.61	11.4	6.74
4.31	1.71	4.56	1.05	3.49	1.61	2.46	1.54

dyke V
ChV1
11
1
114
20
15
bd
10
110
18
1.7
10
68
503
10.4
148
4.1
bd
0.6
bd
bd
1.9
3.4
602
23.6
46.5
4.79
18.1
3.51
0.926
2.83
0.38
1.92
0.37
1.03
0.159
1.04
0.171

2.8
0.29
bd
0.53
14
0.2
10.4
2.02

Heri et al, Fig. 1

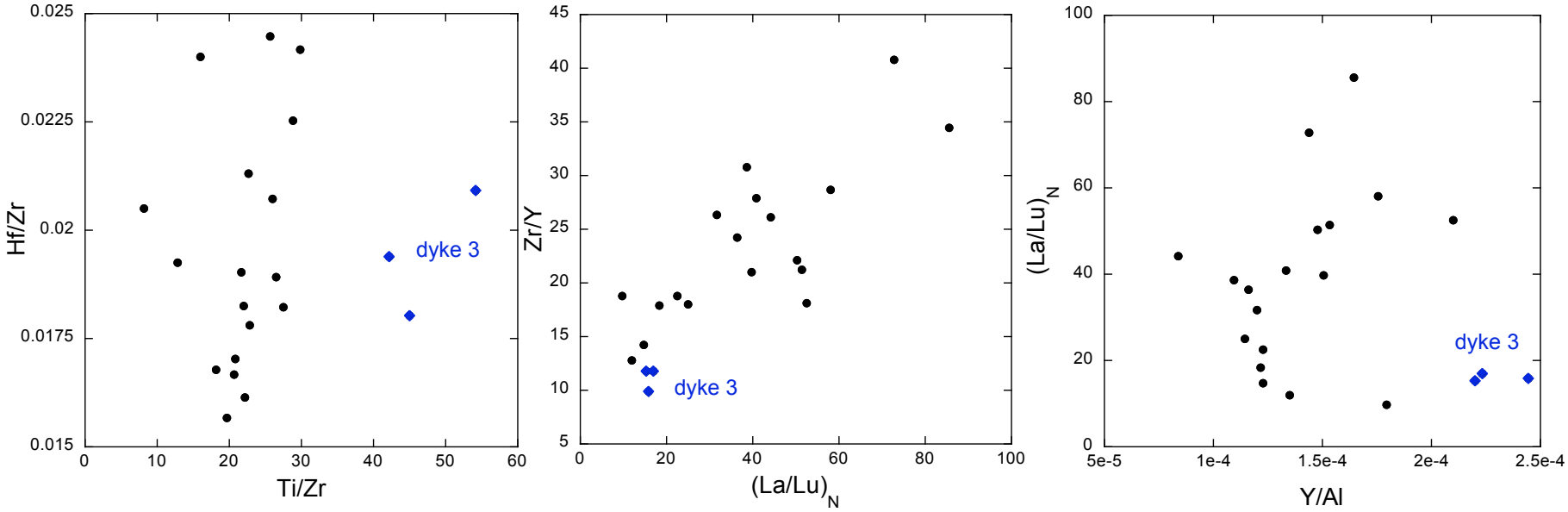

Heri et al., Fig. 2

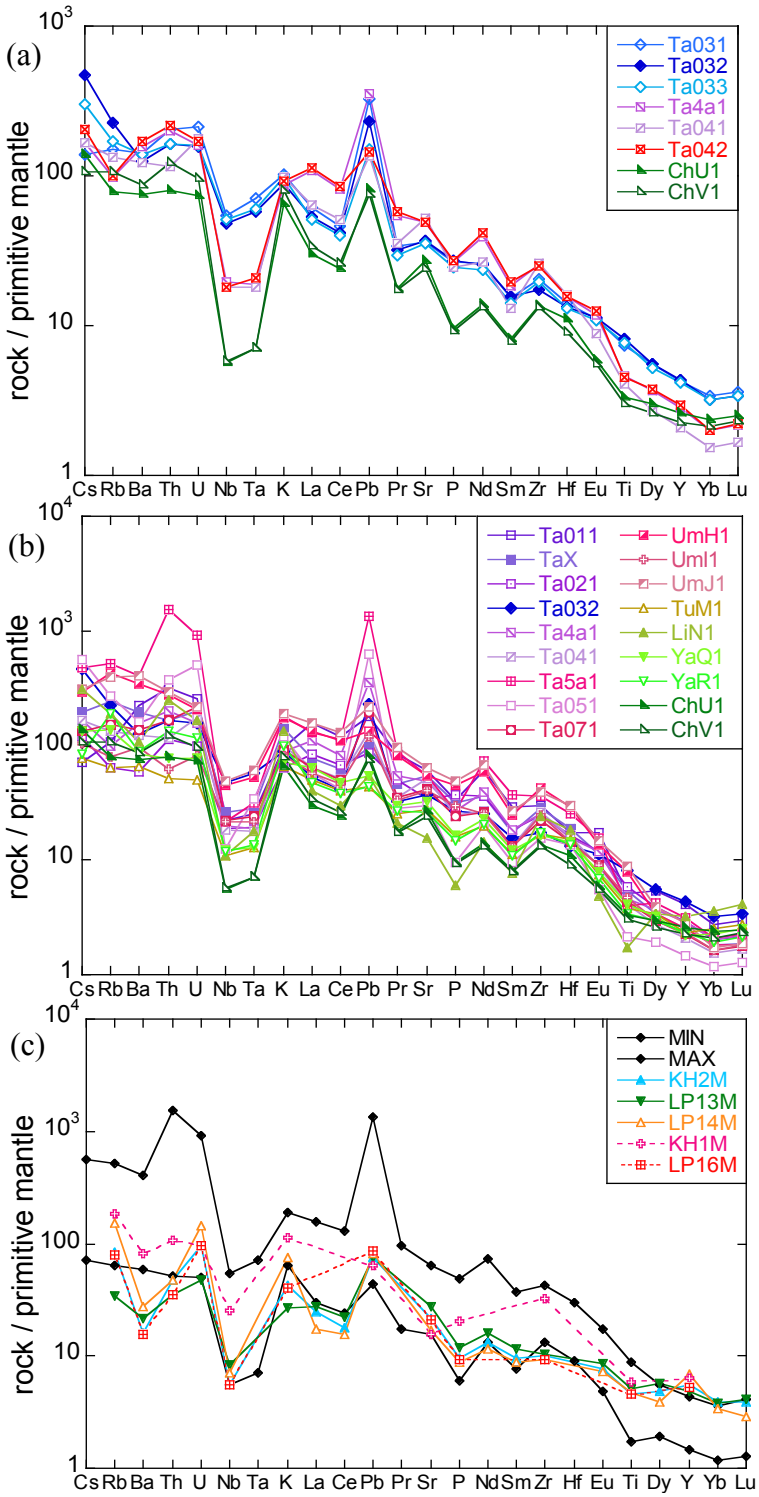

Heri et al., Fig. 3

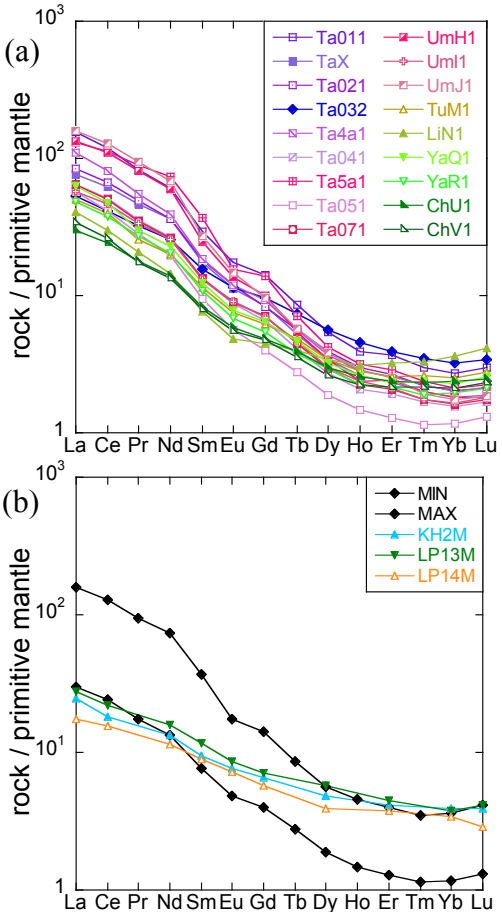

Heri et al., Fig. 4

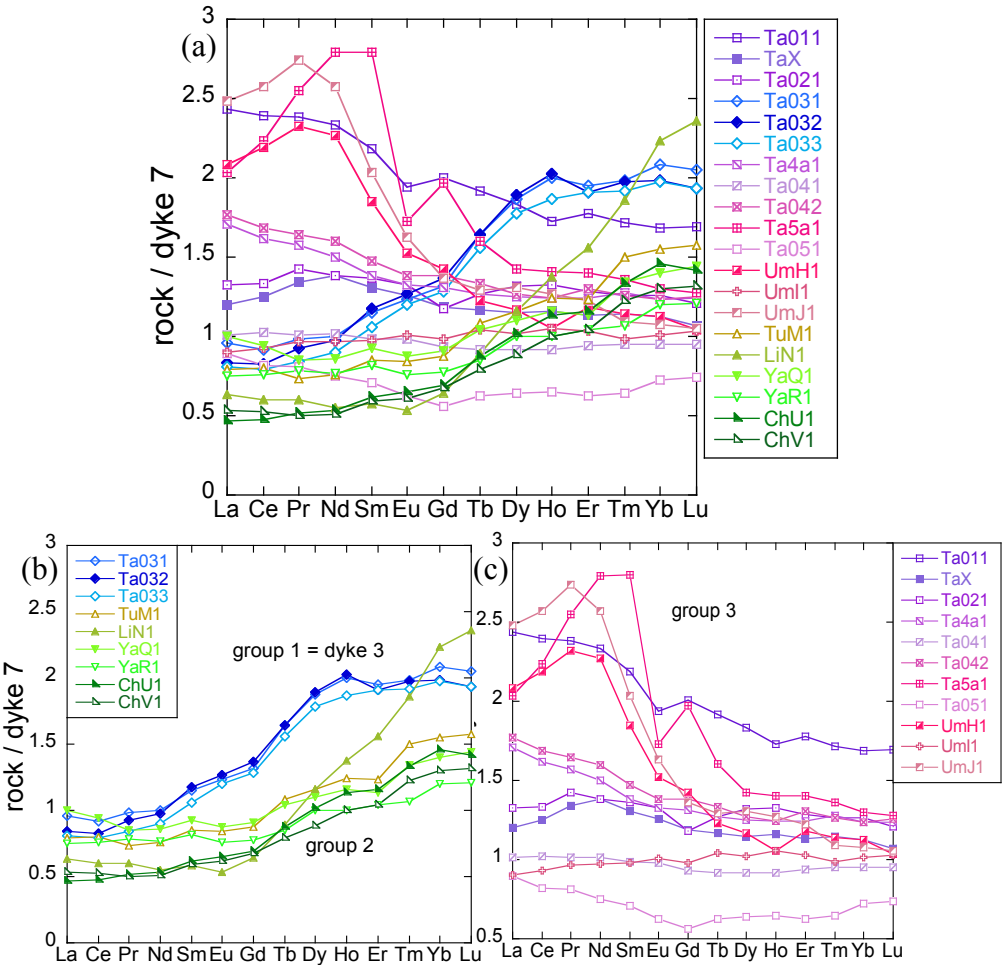

Heri et al., Fig. 5

(a)

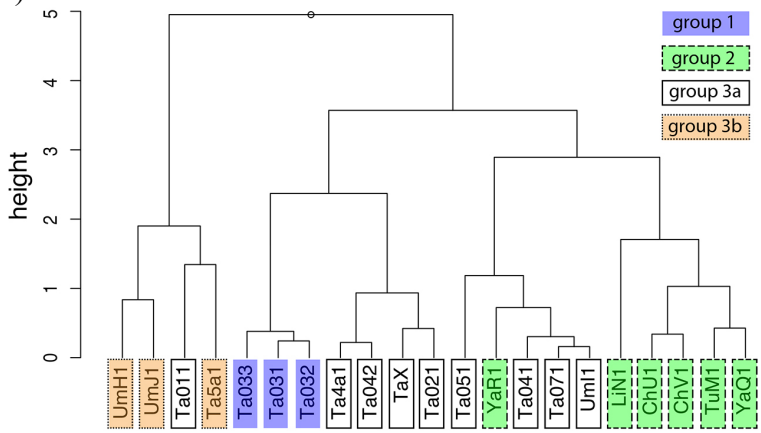

(b)

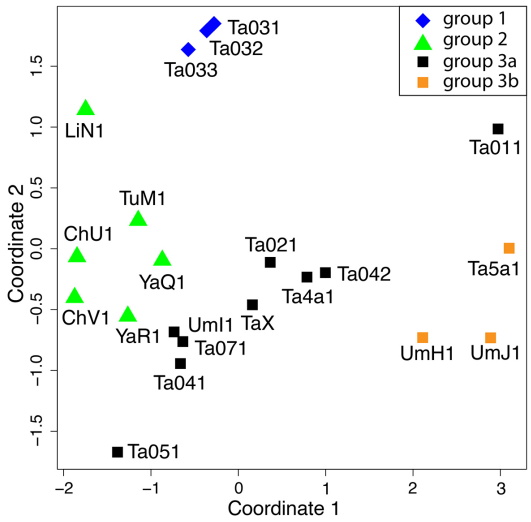

(a)

Heri et al., Fig. 6

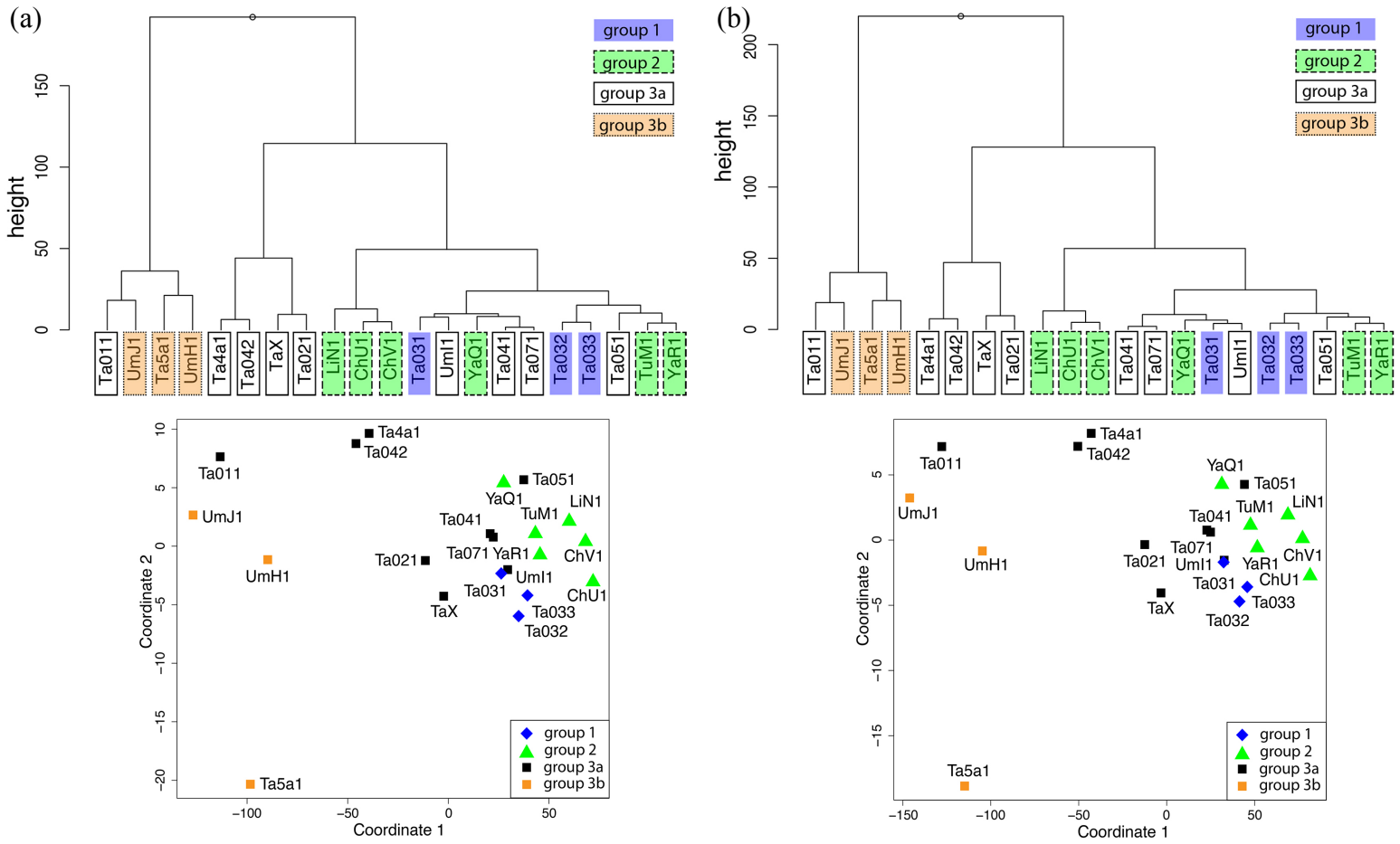

Heri et al., Fig. 7

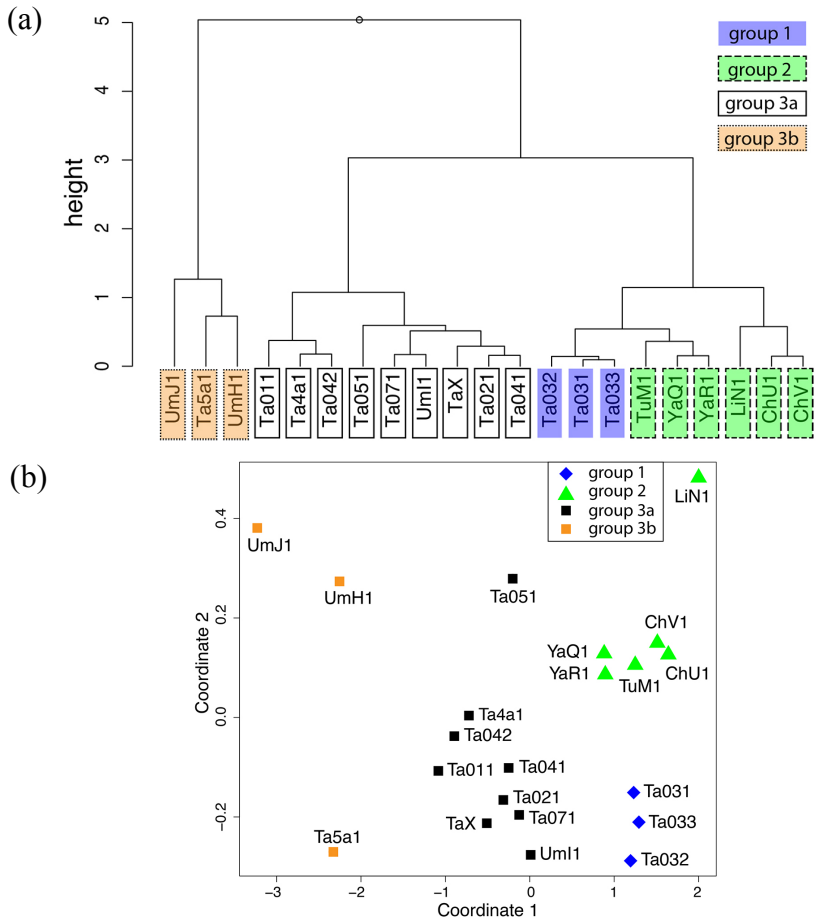

figure

Click here to access/download;figure;Fig.8-R1.pdf

Heri et al., Fig. 8

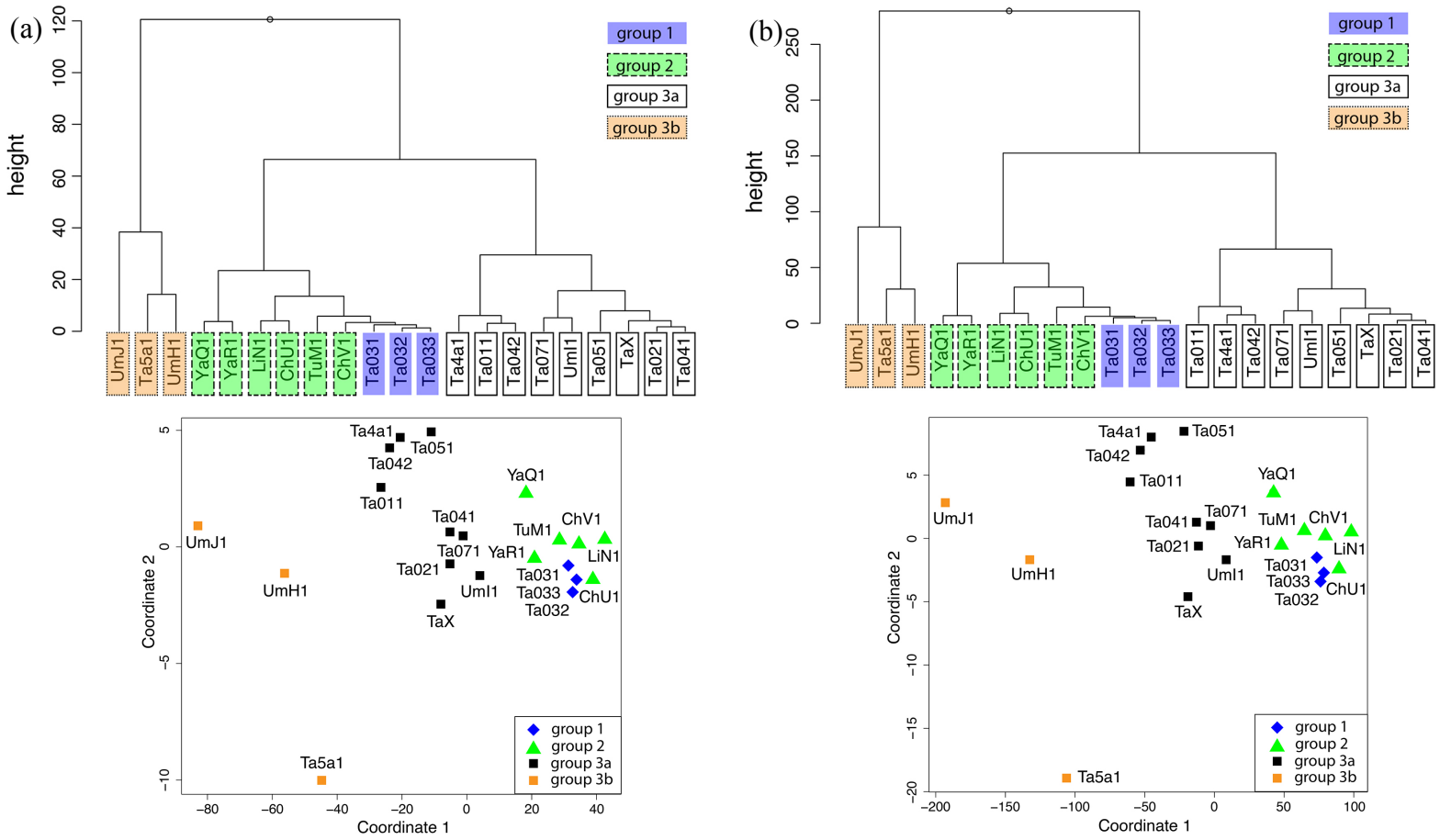

Heri et al., Fig. 9

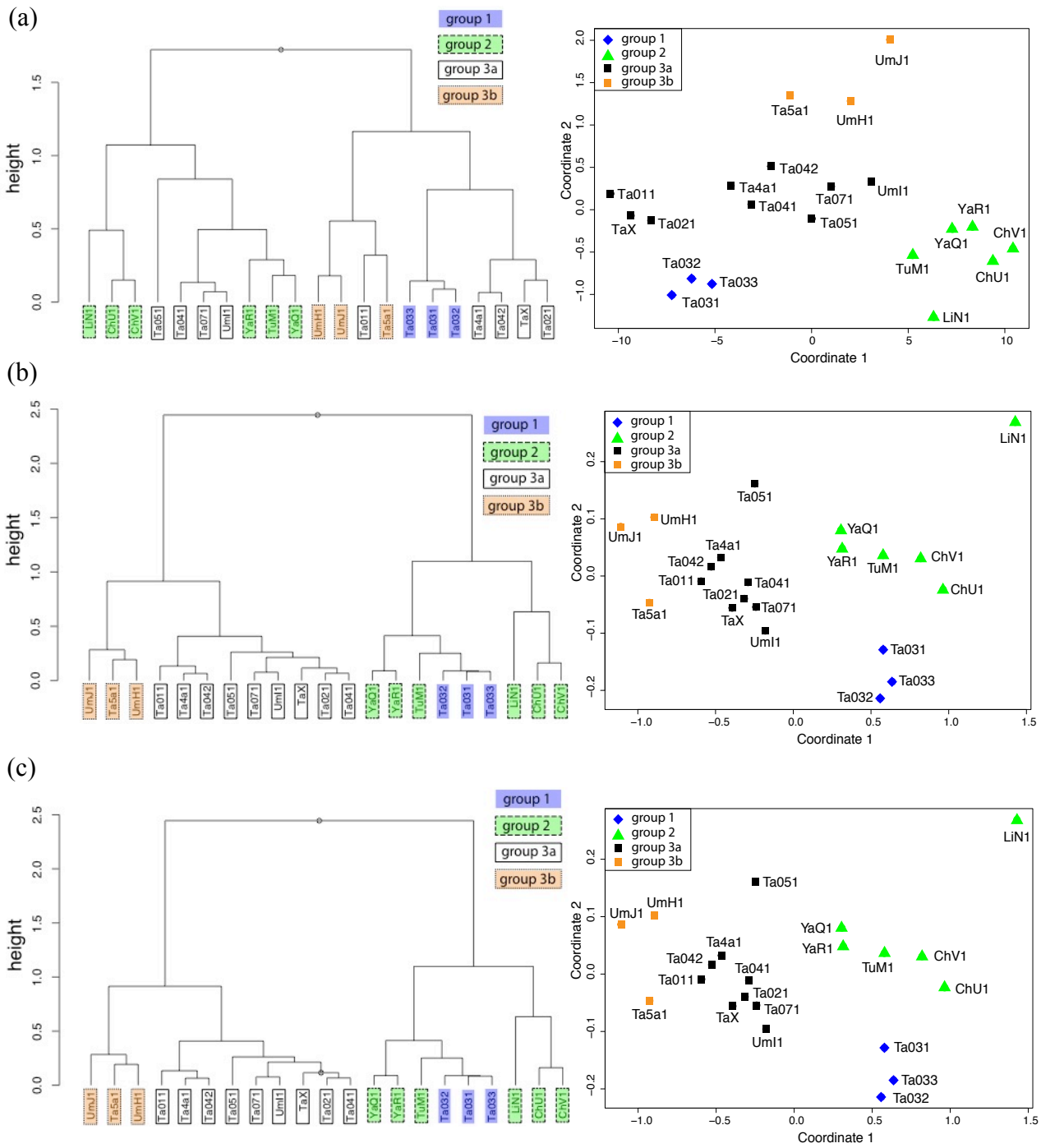

Heri et al., Fig. 10

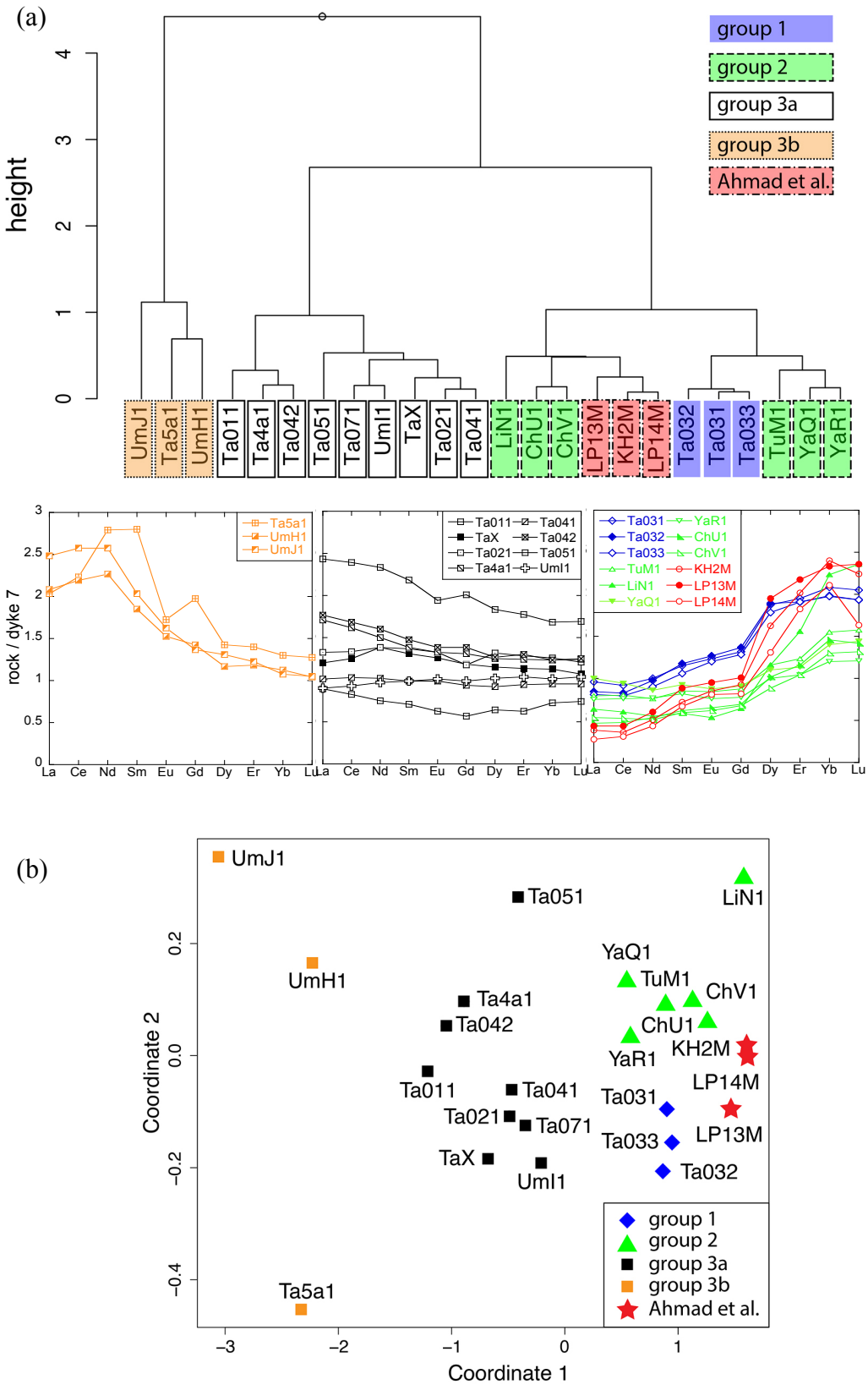

figure

Click here to access/download;figure;Fig.11-R1.pdf

Heri et al., Fig. 11

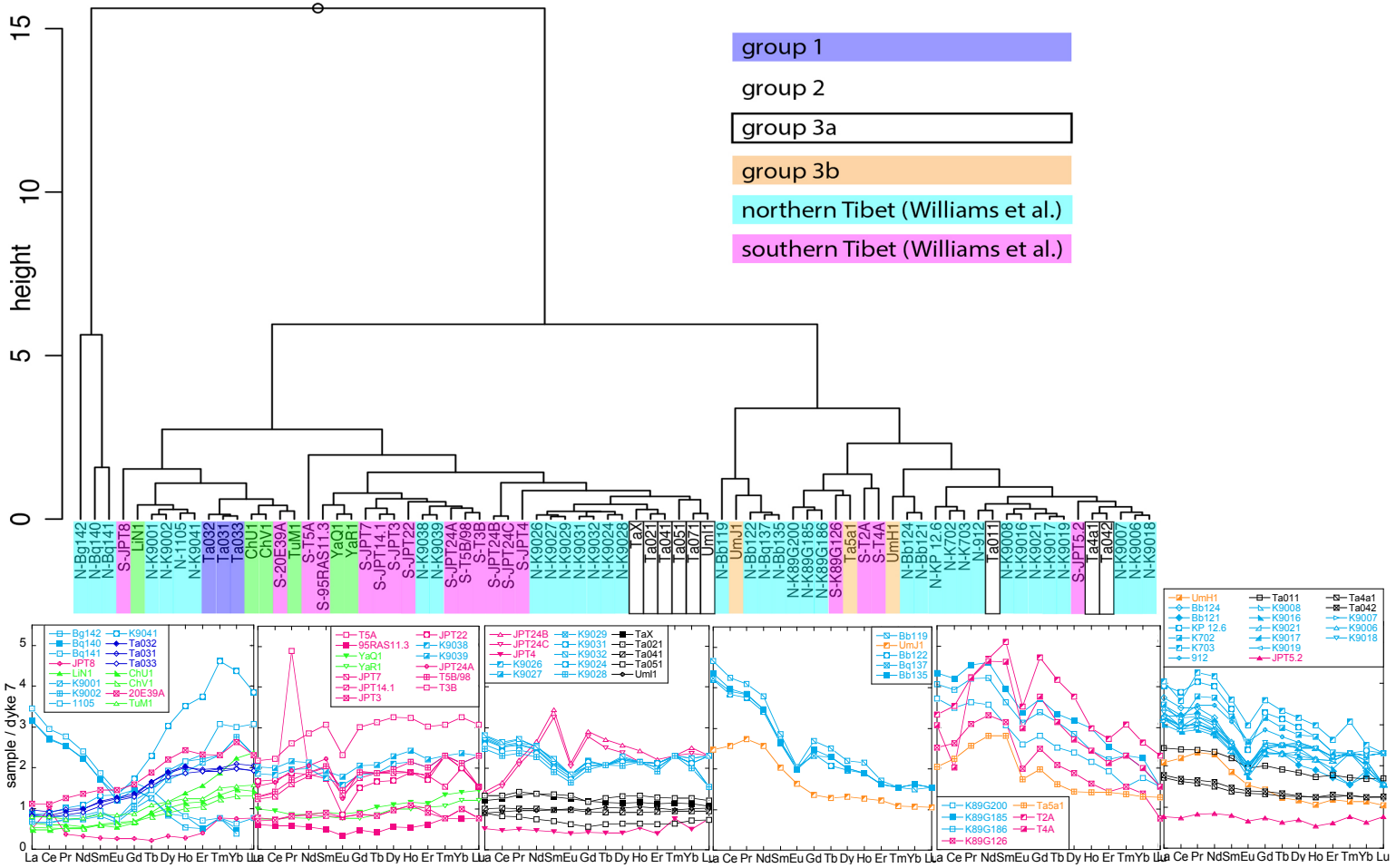

Heri et al., Fig. 12

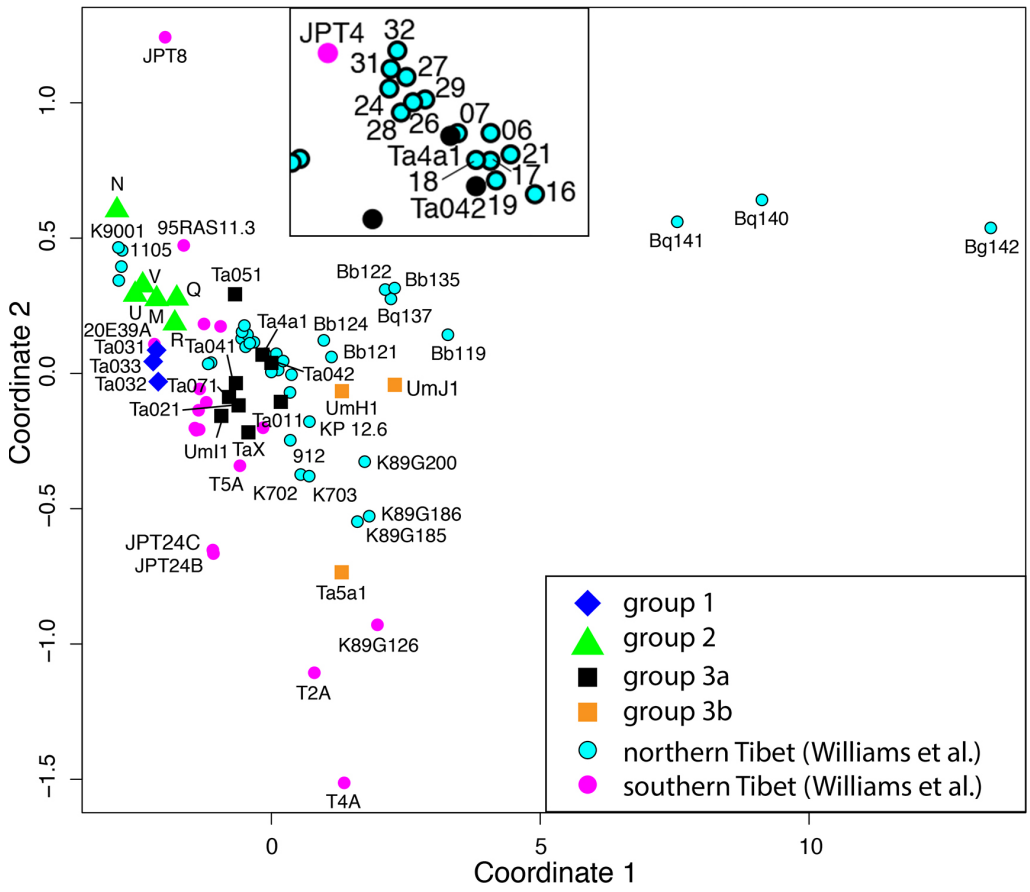

Heri et al., Fig. 13